Gone with the wind: Dune provenance in the northern Rub' al-Khali, United Arab Emirates, Arabia.

Andrew R Farrant*[1], Ian Mounteney[1], Amy Burton[1], Robert J Thomas[2], Nick M W Roberts[3] Robert W O Knox[1†], and Thomas Bide[1].

[1]British Geological Survey, Keyworth, Nottingham, NG12 5GG, UK

[2]Council for Geoscience, Bellville, Western Cape 7535, South Africa

[3]NERC Isotope Geosciences Laboratory, British Geological Survey, Nottingham, NG12 5GG, UK

[†] Deceased.

*Correspondence (arf@bgs.ac.uk)

Abbreviated title: Dune provenance in the northern Rub' al-Khali desert.

Abstract

The Rub' al-Khali dune field in southern Arabia is the largest sand sea in the World. Deciphering the palaeoenvironmental history of the Rub' al-Khali is critical to understanding its role as a barrier to human migration, dispersal and settlement. To determine sediment provenance and transport pathways, we combined geological mapping with traditional heavy mineral optical point-counting methods, heavy mineral geochemical fingerprinting, and detrital zircon U–Pb geochronology of Miocene and Quaternary sediments in the United Arab Emirates (UAE).

Detrital zircon U–Pb age spectra demonstrate that most Neogene and Quaternary sediments in the UAE are ultimately sourced from the Precambrian Arabian Shield. Heavy mineral signatures indicate the dune sands are locally recycled from the deflation of Miocene sandstones and Quaternary siliciclastic palaeodunes exposed along the Arabian Gulf coast, whilst carbonate palaeodunes along the Gulf coast are derived from the deflation of sediments deposited by Tigris-Euphrates River system in the Gulf during Pleistocene lowstands. In the eastern Emirates, Miocene and Quaternary alluvial fan deposits emanating from the Hajar Mountains have an ophiolitic heavy mineral signature. The identification of distinct provenance source signatures coupled with geological mapping reveals new insights into the origin and development of the Rub' al-Khali dune field.

Located at the crossroads between Africa and Eurasia, the deserts of central Arabia occupy a pivotal position for understanding climatic and environmental change in the Late Quaternary. Much of the southern third of the Arabian Peninsula is presently blanketed by the vast Rub' al-Khali dune field (Fig. 1), the largest sand sea in the world. It covers some 650,000 square kilometres, from the Gulf coast of the United Arab Emirates (UAE) south into Saudi Arabia, Oman and Yemen. The sensitivity of this and other Arabian dune fields to environmental change provides us with a powerful tool to understand the enormous changes that have occurred during the Quaternary. Understanding the genesis and evolution of sand seas is critical in understanding how the region evolved during this time,

which in turn has profound implications for models of human occupation, migration and dispersal in Arabia (Parton *et al.* 2015).

Clues to the origin of the Rub' al-Khali dune field are recorded in the detrital sand grains from which the dunes are composed, from Optically Stimulated Luminescence (OSL) and U–Pb detrital zircon age dating (Farrant *et al.* 2012, Farrant *et al.* 2015). However, deciphering this record is not straightforward, principally because the origin of individual sand grains is difficult to determine. In addition, most sand grains have been recycled, sometimes numerous times, from older deposits. Previous studies (Garzanti *et al.* 2003; Garzanti *et al.* 2013) have focussed on determining the ultimate provenance of the dune sands of Arabia through widely dispersed sampling. Whilst these regional, continental-scale studies are extremely valuable in determining the ultimate origin of the sand grains, they are less useful for charting the development of individual dune fields on timescales appropriate to climatic oscillations. By their nature, actively migrating dunes are locally sourced from previous dune forms or local outcrops. To fully assess dune development and provenance, higher resolution studies sampling more local sources of sediment need to be performed to compliment continental-scale studies.

Although the distribution and age of modern dune sands in the northern Rub' al-Khali is well known from previous studies (Glennie & Singvi 2002; Farrant *et al.* 2014), what is less well known is the extent to which locally exposed older rocks have contributed to the development of the dune field. Garzanti *et al.* (2013), for example, suggest that an undetermined and possibly significant amount of the sand in the Jafurah sand sea (Fig. 1) is derived from recycling of the underlying Miocene rocks. The same is likely to be true of the Rub' al-Khali. A thick Miocene succession is exposed along the Gulf coast west of Abu Dhabi and into eastern Saudi Arabia, the upper part of which is predominantly siliciclastic (Whybrow & Hill 1999; Al Safarjalani 2004; Farrant *et al.* 2012; Newell & Farrant 2014). Also exposed across much of the central UAE is a sequence of Quaternary palaeodune sandstones up to 60 m thick (Farrant *et al.* 2014), which extends south into Saudi Arabia. These are often exposed in interdune hollows, and forms the substrate over which the modern dunes now migrate. Extensive deflation associated with the northerly Shamal wind, possibly facilitated by regional uplift (Wood *et al.* 2012; Farrant *et al.* 2014), have exposed these older Miocene and Quaternary palaeodune sandstones along the northern, upwind margin of the Rub' al-Khali desert in the Gulf coast region of the UAE.

To date, the role these sandstones have played in contributing sand to the modern dunes has not been quantified. In this paper we use a range of techniques to determine sediment provenance, coupled with a sampling strategy that includes both local and far-field source rocks. The most reliable method is the use of heavy mineral techniques, principally because the heavy mineral composition is directly related to parent lithology. Moreover, modern desert environments are characterised by a lack of chemical weathering, and physical deterioration is largely limited to fragile lithic components and strongly cleaved minerals such as micas. Nevertheless, most detrital components can survive intact over 10^5-10^6 year timescales (Vermeesch *et al.* 2010). Detrital zircon geochronology is also used as zircons are particularly robust and resistant to multiple cycles of weathering, transport and deposition

(Fedo *et al.* 2003; Gehrels *et al.* 2012). These methods can provide clues to the origin of both modern dunes and potential source rocks, but both have limitations if samples are analysed without understanding the local geological context or relying on widely spaced sample sites.

In this paper, we report on detailed geochemical and heavy mineral provenance studies of modern dune sands and their likely local source rocks from the northern, upwind margin of the Rub' al-Khali desert within the United Arab Emirates. We use a combination of optical counting and geochemical (Inductively Coupled Plasma-Alpha Emission Spectometry; ICP-AES) analyses to characterise the heavy mineral component, coupled with detrital zircon U–Pb dating by Laser Ablation Inductively Coupled Plasma Mass Spectrometry (LA-ICP-MS) to establish the age spectra of the dunes. In doing so, we are able to disentangle the relative contribution of far travelled versus local sediment sources. The results, coupled with an in depth knowledge of local and regional scale geology (Styles *et al.* 2006; Farrant *et al.* 2012) and the geochronology of dune development and stabilisation (Farrant *et al.* 2015) derived from OSL age determinations of dune sand, enable us to better understand how the dunes of the Rub' al-Khali accumulate and evolve in response to shifts in monsoonal patterns driven by orbital parameters, and how this impacts on patterns of human migration and settlement (Parton *et al.* 2015).

Potential sources of sediment

A consideration of regional geology and previous sediment provenance studies in the Arabian Gulf region (Philip 1968; Al-Juboury *et al.* 2009; Al-Juboury & Al-Miamary 2009; Garzanti *et al.* 2013; Garzanti *et al.* 2016) suggest that three potential regional-scale primary sources of sediment can be identified (Fig. 1). These are the Arabian Shield and Platform; the Hajar Mountains; and the Zagros Mountains which feeds sediment into the Arabian Gulf via the Tigris-Euphrates-Karun river system. In addition to these regional sources, several more proximal sediment sources can be identified in the UAE. Each has a distinct heavy mineral signature.

Arabian Shield and Platform

The Arabian plate is bounded to the south by the Red Sea-Gulf of Aden divergent plate boundary, and the Bitlis-Zagros convergent plate boundary to the north, known as the Zagros suture (Fig. 2). The western and eastern margins are marked by the transform faults. Stern & Johnson (2010) and Stern *et al.* (2010) provide comprehensive reviews of the architecture and geological evolution of the Arabian plate. The major part of the Arabian Plate was formed in the Neoproterozoic, after 1000 Ma. The crystalline basement is extensively exposed in the mountains adjacent to the Red Sea uplift and a few scattered outcrops in Oman. It is extensively covered by late Neoproterozoic to Phanerozoic volcano-sedimentary rocks up to 10 km thick (Fig. 1). The Arabian plate is tilted away from the Red Sea uplift, so the cover rocks thicken in a northeasterly direction.

The crystalline basement is divided into two parts (Fig. 2). The western segment, known as the Arabian Shield comprises a succession of Neoproterozoic accreted arc terranes commencing at around 1000 Ma. It underwent orogenesis during the amalgamation of

Gondwana as part of the East African Orogen at around 550 Ma (Stern 1994). Remnants of older, Palaeoproterozoic to Neoarchaean rocks, preserved in southern Saudi Arabia and Yemen, are tectonically interleaved with the Neoproterozoic arc terranes and represent the oldest rocks in Arabia (Whitehouse *et al.* 2001). The geological evolution of the Arabian Shield was essentially only complete by about 550 Ma, so it is covered by relatively thin Phanerozoic deposits.

In contrast, in eastern Arabia (often known as the Arabian Platform) the basement rocks, locally exposed in Oman and entrained in salt domes in the UAE are quite different. Here, the oldest rocks are gneisses with ~1300 Ma protoliths that were deposited at <1000 Ma and intruded by plutonic igneous up to about 720 Ma (e.g. Mercolli *et al.* 2006). Since that time, the Arabian Platform was the site of almost continuous gentle subsidence and sedimentation through the Phanerozoic. Thus, in contrast the Arabian Shield, the Arabian Platform is largely concealed by up to 12 km of Late Neoproterozoic to Phanerozoic cover sequences. The Lower Palaeozoic succession is dominated by quartzose conglomerates, sandstones and siltstones over 3 km thick. The overlying Upper Permian to Cainozoic succession thicken away from the shield to >8 km towards the Gulf where continuous subsidence along the Arabian Neotethys passive margin facilitated the deposition of a thick sequence of clastic and carbonate sediments (Powers *et al.* 1966, Alsharhan & Nairn 1997; Thomas & Ellison 2014).

The sediments derived from the Arabian Shield have a distinctive heavy mineral signature which is dominated by calcic-amphibole and epidote, with moderate amounts of clinopyroxenes (predominantly augite), garnet and zircon, and minor amounts of orthopyroxene (predominantly enstatite), rutile, titanite and tourmaline. The highly mature Lower Palaeozoic quartz arenites that crop out along the eastern margin of the Arabian Shield have a heavy mineral assemblage dominated by the ultra-stable phases - zircon, tourmaline and rutile. Less stable accessories – apatite, staurolite and garnet – are probably sourced from the 'Pan-African' basement (Bassis *et al.* 2016).

The Zagros Mountains and Arabian Gulf

The Zagros Mountains are a major NW-SE trending thrust and fold belt created during the collision of the Eurasian and Arabian plate during the closure of the Neothys Ocean (Fig. 1). This started in the Eocene at around 50 Ma and culminated during the Miocene (Mouthereau *et al.* 2012). The collision continues to this day and the area remains seismically active. The mountains are dominated by a >10 km thick succession of Palaeozoic to Cainozoic, largely platform-carbonate sedimentary strata originally deposited on the Arabian continental margin (Garzanti 2013). Orogenic detritus from the uplifted Zagros Mountains is routed via rivers into the Arabian Gulf, the largest of which is the Tigris-Euphrates-Karun system. These fluvial systems have been the dominant allogenic source of sediment into the Arabian Gulf foreland basin. There is little or no terrigenous input from the Arabian side of the Gulf, and most modern sediment deposition is dominated by carbonate.

The heavy mineral assemblage associated with the Tigris and Euphrates sediments are reported to contain magnetite, chromite, haematite, ilmenite, goethite and pyrite, and non-opaques including epidote, pyroxenes, amphiboles, garnet, zircon, tourmaline, rutile, kyanite, staurolite, olivine, titanite and apatite (Philip 1968; Al-Juboury *et al.* 2009; Al-Juboury & Al-Miamary 2009; Garzanti *et al.* 2013; Garzanti *et al.* 2016). This heavy mineral assemblage reflects the input of mafic and ultramafic igneous rocks, metamorphic and ophiolitic sequences of northern Iraq and southern Turkey. High Cr and Ni values in the Tigris sediments in northern Iraq are potentially sourced from the ophiolite-radiolarite belt of the Taurus Range (Aqrawi & Evans 1994; Al-Juboury *et al.* 2009). Aeolian sands in southern Iraq are characterized by large amounts of opaque and unstable minerals of the hornblende, epidote, and pyroxene groups (Skoček & Saadallah 1972), similar to sediments of the Lower Mesopotamian Plain.

During glacial low sea-level stands during the Pleistocene (Lambeck 1996), the floor of the Arabian Gulf is believed to have been exposed. During these low-stands, the Tigris-Euphrates river system would have prograded along the axis of the Gulf depositing fluvial and overbank sediment which would have been prone to deflation and thus available as a potential source of sediment. These Gulf-derived sediments thus have a distinctive Tigris-Euphrates signature.

Hajar Mountains

The Hajar Mountains (Fig. 1), straddling the UAE-Oman border are dominated by two major units: the Oman-UAE ophiolite; and in the north, an uncomformable Mesozoic platform carbonate sequence (Styles *et al.* 2006). The Oman-UAE ophiolite formed during the obduction of Tethyian oceanic crust onto the eastern Arabian margin during the Late Cretaceous at *c.* 96 Ma (Goodenough *et al.* 2014; Roberts *et al.* 2016). The ophiolite is immediately underlain by a metamorphic sole (e.g. Searle *et al.* 2014), comprising moderate- to high-grade, polydeformed metasedimentary and meta-igneous rocks. The Hajar Mountains were formed during subsequent exhumation events related to the Zagros Orogeny at ~45 to 35 Ma and 20 to 15 Ma (Jacobs *et al.* 2015). The thrusting and folding of the underlying sediments was followed by the development of a foreland basin west of the Hajar Mountains that was filled by a Late Cretaceous to Palaeogene cover sequence dominated by nummulitic limestones, mudstones and evaporites. Later thrusting and folding affected both the Mesozoic and Palaeogene sedimentary sequences and led to the formation of a Neogene foreland basin, subsequently infilled with altered dolomitised detrital ophiolitic sediments (Lacinska *et al.* 2014).

The mafic, ultrabasic and metamorphic rocks give rise to a distinctive heavy mineral assemblage characterised by magnetite, chromite, hematite, ilmenite, goethite, epidote, pyroxenes (augite and enstatite), amphiboles, garnet, zircon, tourmaline, rutile, kyanite, staurolite, olivine, titanite and apatite (Garzanti *et al.* 2003; 2016).

Local source rocks: Miocene and Quaternary sediments of the UAE

In addition to the regional sediment sources, weakly-cemented Miocene sandstones and Quaternary deposits along the northern and eastern margins of the Rub' al-Khali are actively

being deflated and supplying aeolian sediment to the dune-field (Fig. 3). The heavy mineral signature of these local sources are examined in this study.

Miocene rocks crop out along the coast between Abu Dhabi and Qatar, in eastern Saudi Arabia, along the western flank of the Hajar Mountains, and in deflation hollows within the dune-field. These rocks comprise a carbonate succession, (the Dam and Ras Khumais formations (Dill *et al.* 2005; Farrant *et al.* 2012; Newell *et al.* 2012)), overlain by a siliciclastic sequence. Four major siliciclastic units are currently exposed in the UAE (Fig. 3). In the west, the Miocene siliciclastic succession is divided into two units, the Shuwaihat and Baynunah formations. The Shuwaihat Formation (Bristow & Hill 1998) consists of fluvial, dune and playa sandstones and mudstones up to 20 m thick, although locally it is much thinner. The Baynunah Formation comprises a sequence of fluvial sandstones typically around 40 to 60 m thick (Whybrow & Hill 1999). A fossiliferous intraformational conglomerate at the base fines up to fluvio-lacustrine sandstones and siltstones at the top (Farrant *et al.* 2012). Both the Shuwaihat Formation and the lower part of the Baynunah Formation are characterised by fluvial systems with channels approaching 100 m in width.

East of Abu Dhabi, the Miocene Baynunah and Shuwaihat formations thin and merge with the fluvial sandstones, conglomerates and dolomitic mudstones of the Barzaman Formation. This formation is dominated by clasts of ophiolitic igneous material (harzburgite and gabbro), along with chert and limestone derived largely from the Hajar Mountains. The sediments have been extensively replaced by dolomite generated by the diagenetic alteration of harzburgite to carbonate (Lacinska *et al.* 2014). The formation forms a prograding clastic wedge up to 400 m thick in the east, extending out and thinning into the foreland basin as far west as Abu Dhabi.

The coarse-grained pebbly fluvial sandstones of the Pliocene-Quaternary Hofuf Formation crop out in the far west of the UAE. Although only a few metres thick in the UAE, it thickens rapidly to the west and attains a thickness of about 95 m (Al Safarjalani 2004) across the Eastern Province of Saudi Arabia (Hofuf and Haradh). The heavy-mineral assemblage of the Hofuf Formation is characterized by abundant unstable minerals, particularly hornblende, pyroxene and epidote (Al-Saad *et al.* 2002).

Younger Quaternary palaeodune and alluvial fan sediments underlie much of the northern Rub' al-Khali. Overlying the Miocene succession with a strongly erosive unconformity are two major palaeodune sequences (Fig. 3); the Madinat Zayed and the Ghayathi formations (Farrant *et al.* 2012). The Madinat Zayed Formation is the thickest and most extensive, underlying much of the modern dune field across the central and western UAE. This predominantly quartzose sandstone is up to 60 m thick. It is exposed by deflation in a narrow zone around the northern, upwind edge of the Rub' al-Khali, but extends south beneath the modern dune field at least as far south as the Liwa oasis. By contrast, the Ghayathi Formation is a predominantly carbonate sandstone consisting largely of well-rounded bioclasts. It crops out sporadically along and just inland from the Gulf coast between Ras al Khaimah and Ruwais, particularly between Abu Dhabi and Dubai. It has a very variable thickness, typically between 1-10 m.

To the east, extensive Quaternary alluvial fan deposits extend out from the Hajar Mountains to Abu Dhabi. These deposits, termed the Hili Formation (Styles *et al.* 2006) are known to be greater than 40 m thick near Al Ain (Parton *et al.* 2015) and thin westwards. They consist of a lithologically variable unit of ophiolitic conglomerates, quartzose sands (predominantly fluvially reworked aeolian sand) and silts that represent the distal component of the drainage systems that emanate out from the Hajar Mountains as far as Abu Dhabi. These sediments were deposited in a series of now relict alluvial fans, distal sandy braid-plain and wadi environments. It is the lateral equivalent of the Madinat Zayed Formation; with which it merges. In the northern Emirates, the alluvial fans are dominated by locally-derived limestone clasts with little sand.

In the far west of the UAE, a thin, pebbly sand unit overlies the Miocene sediments in Sabkha Mati. These gravelly sands (Sabkha Mati gravels) are probably derived from the Hofuf Formation to the west. Along the Gulf coast between Dubai and Ruwais are sporadic, isolated outcrops of raised marine limestones, termed the Fuwayrit Formation. These Quaternary deposits are typically bioclastic grainstones that cap low zeugen of the underlying Ghayathi Formation (Williams & Walkden, 2002; Wood *et al.* 2012; Farrant *et al.* 2012) and are restricted to within a few kilometres of the present coastline.

Methods

In order to characterise the heavy mineral composition of the Rub' al-Khali dunes 194 sand samples of both active dunes and potential source rocks were collected from multiple sites across the UAE, typically 100-150 g each (Fig. 3 and Supplementary data). These include active dunes, palaeodunes, fluvial deposits, raised marine sediments and Miocene sandstones. For modern dunes, samples were collected from dune crests to avoid anomalous concentrations of denser minerals. Particular care was taken to collect representative samples from each of the underlying geological units. In addition, modern dune samples were collected along two transects: one downwind from the Gulf coast to the Liwa oasis, and one from Abu Dhabi east to the Hajar Mountains (Fig. 3). Of the 194 samples collected, 193 were analysed for bulk heavy-mineral geochemistry and 146 were counted using traditional optical microscopy. For the U–Pb zircon geochronology study, seven larger (>1 kg) samples were collected, again from both Quaternary dunes and palaeodunes, and from the underlying Miocene sandstones.

Heavy media separation

Subsamples ranging from 100-200 g were taken, dispersed in deionised water and shook overnight to aid in the disaggregation of sand, silt and clay. Following dispersion, the 63-125 µm fraction was wet sieved following Morton & Hallsworth, (1994), and the heavy minerals separated using typical sink float method using lithium heteropolytungstate (adjusted to 2.8 g/cm^3). Zircons for the U–Pb study were treated separately form the heavy mineral study and extracted from the seven samples using different techniques as outlined below.

Optical identification/counting

For optical microscopy of the heavy minerals, the mineral concentrates were mounted onto a standard glass slide using a petropoxy resin, cover-slipped and cured overnight. Heavy mineral counting was performed using a standard ribbon-counting method (Garzanti *et al.* 2013). An average of 600 transparent detrital heavy minerals were counted per sample. Mineral indices were established from the calculation of selected mineral pairs. These indices are designed to compare the relative abundance of minerals that possess similar hydraulic properties. For provenance purposes, the indices are normally based on minerals such as zircon and rutile that are stable under all conditions of weathering and burial depth and whose relative abundance is thus broadly representative of their relative abundance in the source rocks (Morton & Hallsworth 1994). Ratios based on these minerals provide the most reliable means of discriminating between sands of different provenance. Two appropriate mineral indices defined by Morton (1985) were applied to sediments from the UAE: the rutile:zircon index (RZi) and the chrome-spinel:zircon index (CZi). All mineral indices are calculated according to the formula:

100 x (mineral 1 count)/(mineral 1 count + mineral 2 count).

Indices based on less stable heavy minerals are reliable as provenance indicators only if it can be demonstrated that they have not been substantially affected by dissolution, either by surface pore waters (weathering) or subsurface pore waters (diagenesis).

Heavy mineral geochemistry by ICP-AES

For the bulk heavy-mineral geochemistry (Mounteney *et al.* 2017, in press) the remaining heavy mineral concentrate was micronised to further reduce the particle size to <20 µm. A 0.1 g subsample was placed into a platinum crucible with 0.9 g lithium metaborate flux and mixed thoroughly. Samples were flash-fused at 1050 °C for 15 minutes. Once cool, the crucibles were placed into capped vessels containing 50 ml MQ water, 5 ml nitric acid (HNO_3) and 1 ml hydrofluoric acid (HF), and placed on a shaker overnight. After 18 hours, an additional 44 ml MQ water was added to the vessels prior to analysis. Geochemical analysis was performed using a Perkin Elmer 7300 DV ICP-AES for a suite of 27 major and trace elements.

U-Pb geochronology

Zircons were separated using standard techniques (Wilfley table, Frantz magnetic separator, Heavy liquids). An aliquot of each sample was mounted in a 1-inch epoxy mount without picking to avoid biased selection. Each mount was polished to expose the zircon interiors, and then imaged with a Scanning Electron Microscope (SEM) using cathodoluminescense (CL) to guide spot location. U-Pb analyses were performed at NIGL (Nottingham) using a New Wave Research (ESI) 193FX Excimer laser ablation system coupled to either a Nu Instruments Nu Plasma multi-collector ICP-MS or a Nu Instruments Attom single collector ICP-MS. See Roberts *et al.* (2011) and Thomas *et al.* (2013) for full descriptions of the methods. The analytical set-up and full dataset is available in the online supplementary files. Age uncertainties are quoted at 2σ and are propagated following Horstwood *et al.* (2016).

Sample mineralogy.

The detrital heavy-mineral assemblages in all the samples (Miocene, Quaternary and modern) are documented in the supplementary data. They are dominated by ferromagnesian minerals (average 73.5%) (Fig. 4). These include epidote (Ep), averaging 35.7%, calcic amphibole (Ca - 25.8%), clinopyroxene (Cpx - 6.8%) and orthopyroxene (Opx - 3.4%). The other major constituent is garnet (Grt - 12.6%). All of these minerals are susceptible to dissolution during both weathering and burial-related diagenesis, with pyroxene and amphibole the most unstable. Of the 146 samples which were analysed optically, 39 samples showed evidence of preferential dissolution; this was identified by the development of hacksaw terminations of pyroxene (enstatite) (Fig. 5b) and amphibole (hornblende) (Fig. 5d). The 39 samples that displayed evidence of selective dissolution were predominantly located along the coast of the UAE. However, the relatively young age of the sediments combined with the hyper-arid conditions and the lack of any substantial burial or diagenesis precludes significant preferential dissolution of pyroxenes and amphiboles (Andò *et al.* 2012). The remaining minor components of the averaged heavy mineral assemblages includes: apatite (Ap) 1.1%, Cr-spinel (Chr) 3.0%, rutile (Rt) 1.2%, staurolite (St) 0.5%, titanite (Ttn) 1.5%, tourmaline (Tur) 3.1% and zircon (Zrn) 4.3%. The remaining 1% of the averaged heavy mineral component includes trace quantities of the minerals andalusite (And), brookite (Br), glaucophane (Gln) kyanite (Ky), monazite (Mnz), silliminite (Sil) and blue-green spinel (Spl).

Provenance signatures were established through the comparison of minerals with similar physical properties. Mineral data were normalised based on their minima and maxima to produce a comparable set of data (Kumar-Jain & Bhandare, 2011). Mineral plots are used to differentiate geological units based on ultra-stable and less stable components. These are further-divided into mineralogical and geochemical data (Fig. 6). Less-stable minerals (LSM) including orthopyroxene, clinopyroxene and calcic-amphibole (Fig. 6a), ultra-stable minerals (USM) including Cr-spinel, rutile+titanite and zircon (Fig. 6b), less-stable mineral geochemistry (LSMG) including Ca, Fe and Mg (Fig. 6c) and ultra-stable mineral geochemistry (USMG) including Cr, Ti and Zr (Fig. 6d). The rutile:zircon (RZi) and the chrome-spinel:zircon (CZi) indices as used by Morton & Hallsworth (1994) are shown in Fig. 7, whilst the grain size distribution of samples is shown in Fig. 8. The heavy mineral data derived from both optical counting and geochemical data from ICP-AES clearly demonstrate that there is a systematic difference in the provenance signature for certain groups of samples, whilst others display a more mixed signature. These are discussed below.

4.1 Miocene to Pliocene sediments

The average heavy mineral component of the Miocene Baynunah and Shuwaihat formations are displayed in Fig. 4. There appears to be very little discernible difference between the heavy mineral assemblages of both formations and they have a proportionally-similar average mineralogy. Because there appears to be very little compositional variability between the two formations, they have been grouped as a single ‘Miocene’ entity. The bulk of the Miocene samples show a distinct grouping. However, a cluster of four samples from the Baynunah Formation (UAE 7847, 7851, 7981 and 7986) are distinct from the rest. They appear comparatively enriched in Mg (Fig. 9a) and Cr (Fig. 9b). Three of these four samples

(UAE 7847, 7851 and 7981) also have increased orthopyroxene (28.7%, 19.1% and 18.8% respectively). These are represented as a small cluster of three Miocene samples in the LSM plot (Fig. 6a). The CZi:RZi comparison (Fig. 7) clearly distinguishes the Miocene samples which all have CZi values of <35.

4.2 Ghayathi Formation

The Ghayathi Formation, whilst dominated by carbonate bioclasts does contain a small component of siliciclastic material. The heavy mineral assemblage in the siliciclastic component (Fig. 4) is dominated by calcic-amphibole and epidote, with moderate clinopyroxenes (predominantly augite) and garnet, with minor amounts of apatite, orthopyroxene (predominantly enstatite), rutile, titanite, tourmaline and zircon. It is characterised by higher RZi and high CZi values (Fig. 7). The LSM (Fig. 6a) is dominated by calcic-amphibole and clinopyroxene with little orthopyroxene. The corresponding LSMG (Fig. 6c), shows a discrete population with coequal concentrations of Ca, Fe and Mg. The USM (Fig. 6b) component of the Ghaythi Formation shows a bias towards Cr-spinel which is also reflected in the USMG (Fig. 6d).

4.3 Sabkha Mati

The Sabkha Mati gravels are a suite of deflated and reworked fluvial sands. The average heavy mineral component (Fig. 4) has the highest average concentration of calcic-amphibole. The heavy mineral assemblage is very similar to the Miocene sediments with a heavy mineral component reduced in Cr-spinel (Fig. 6b), and a LSM biased towards calc-amphibole (Fig. 6a). The corresponding USMG (Fig. 6d) also plots the Sabkha Mati Formation firmly within the cluster of Miocene sediments.

4.4 Limestone fans

In the NE of the UAE, the alluvial fans which emanate out of the mountains around Ras al Khaimah are composed largely of limestone clasts. The average heavy mineral component (Fig. 4) has the lowest average concentration of calcic-amphibole. This heavy mineral assemblage is analogous to Ghayathi Formation, with a similar USMG signature (Fig. 6d) and LSMG (Fig. 6c). They are also more dominant in clinopyroxene and calcic-amphibole (Fig. 6) and with a CZi of 60-90 (Fig. 7), akin to the Ghayathi Formation.

4.5 Madinat Zayed Formation

The average heavy mineral component of the Madinat Zayed Formation is displayed in Fig. 4. The LSM component (Fig. 6) is predominantly calcic amphibole with moderate clinopyroxene. The associated LSMG shows a discrete cluster of samples slightly biased towards a ferro-calcic signature. There is, however a clear subdivision into two distinct populations. This is best defined in the USMG (Fig. 6d) but is also apparent in the USM (Fig. 6c). One population has a similar signature to the Miocene group sediments (biased towards Ti and Zr); the second population is biased towards Cr/Cr-spinel.

4.6 Hili Formation

Much of the Hili Formation consists of coarse ophiolitic conglomerates, with clasts of harzburgite, gabbro and chert, together with some limestone clasts, interbedded with finer-grained sandstone units. The Hili Formation has the highest average concentration of orthopyroxene (Fig. 4). The LSM is biased towards orthopyroxene and calcic-amphibole, the associated LSMG is biased towards a ferromagnesian signature. The USM component is more distinctive in the geochemistry (Fig. 6) with a well-defined population biased towards Cr.

4.7 Fuwayrit Formation

The raised marine limestones of the Fuwayrit Formation typically comprise grainstones dominated by ooids and other bioclasts. Like the Ghayathi Formation, the Fuwayrit Formation has a minor siliciclastic component. The heavy mineral signature (Fig. 4) is analogous to the Ghayathi Formation, however, the CZi and RZi (Fig. 7) are generally higher with CZi of >67 and RZi >35. The particle size distribution (Fig. 8) is predominantly coarse grained (> 125 µm).

4.8 Modern dunes

Across the UAE, there is a marked progressive change in both colour and mineralogy of the dune sands between the coast and the interior. Sands along the Gulf coast are typified by pale beige, fine- to medium-grained, poorly-sorted, compositionally immature, moderately texturally mature carbonate sand containing a small proportion (up to *c.* 10 modal %) of siliciclastic sand-grade debris. The dunes to the south, including the large megabarchans of the Liwa, comprise darker reddish-orange-brown iron-coated, quartz-dominated fine sand. This change has previously been attributed to either the progressive decrease inland in the amount of carbonate-rich bioclastic sand ('Gulf' sand) from the Arabian Gulf (Teller *et al.* 2000), or to the decreasing component of sand derived from the Zagros Mountains (Garzanti *et al.* 2003).

As is expected with an aeolian environment there are associated degrees of mixing between sand types, this is reflected by the broad overlapping dune sand populations (Figs 6 and 7). A distinct unique population can be identified from the LSMG (Fig. 6c) which is comparatively Fe depleted, ~50% Ca and ~50% Mg. The particle size distribution of the dune sands (Fig. 8) is also predominantly coarse-grained (> 125 µm) due the removal of fine grained siliciclastic and carbonate cements from the host formations. This also implies that there has been minimal attrition of grains from aeolian transport.

Detrital zircon geochronology

U-Pb detrital zircon data from seven samples (Table 1) of Miocene and Quaternary sediments were obtained in order to establish the age of provenance of the sediments within the wider Middle East tectonic framework. The data are illustrated in Fig. 10 as Kernel Density Estimates (KDEs) with associated histograms, plotted using DensityPlotter (Vermeesch 2012). The youngest $^{206}Pb/^{238}U$ ages of each sample are quoted for comparison. These do not represent robust maximum deposition ages since they reflect single analyses

from single zircons, and such data are subject to some uncertainty relating to young lead-loss (see Spencer *et al.* 2016).

Miocene Shuwaihat Formation (UAE_6380)

On palaeontological grounds, the Miocene Shuwaihat Formation is thought to have been deposited at ~12 Ma. U-Pb data are mostly concordant (95 out of 97 grains analysed were within 5% of concordance, and 95 within 10%). Ages range in age from earliest Cambrian (c. 530 Ma) to Neoarchaean (2690 Ma). Age maxima are present at: *c.* 540, 610, 780, 860, and 940 Ma, with 51 grains falling within the Neoproterozoic between *c.* 530 and 650 Ma. A robust estimate of the maximum age of deposition of the sample is based on the youngest five ages at 540 ± 5 Ma (weighted mean $^{206}Pb/^{238}U$ age; MSWD =1.1). The youngest concordant single zircon has a $^{206}Pb/^{238}U$ age of 532 ± 13 Ma.

Miocene Baynunah Formation (UAE_7422)

A sample of weakly cemented reddish brown sandstone from the lower part of the Baynunah Formation gave mostly concordant zircon data with 102 of 115 grains analysed being less than 10% concordant. The youngest grain measured had an age of 8 ± 0.2 Ma. This youngest grain is significant and speculatively constrains the maximum age of deposition of the Baynunah Formation to 8 Ma. It is much younger than the youngest grains from the underlying Shuwaihat Formation, and also implies that somewhere in the provenance area there are, as yet unrecognised, igneous (volcanic or volcanoclastic) rocks of this age. The sample also contains other post-Cambrian zircons at *c.* 45 (Palaeocene, 1 grain), *c.* 166 to 178 (Jurassic, 3 grains) and *c.* 312 Ma (Carboniferous, 1 grain). As with the Shuwaihat Formation sample, there is a major Neoproterozoic peak at *c.* 630 Ma (23 grains), forming the core of a major grouping of Late Neoproterozoic zircons between 529 and 692 Ma (53 zircon grains). Other Early Neoproterozoic zircons are seen between *c.* 703 and 968 Ma, with maxima at *c.* 810 and 860 Ma. The sample contains 5 Late Mesoproterozoic grains between *c.* 1000-1120 Ma. Older sources are sparse, with one grain each at *c.* 1617 and 1978 Ma (Palaeoproterozoic) and *c.* 2518, 2694 and 2808 Ma (Neoarchaean).

Quaternary Madinat Zayed Formation (UAE_7007, UAE_7013)

Two typical samples of the Madinat Zayed Formation were selected for analysis. Sample UAE_7007 is an aeolianite while UAE_7013 is a fluvial sandstone. In sample UAE_7007 the youngest concordant zircon (77 of 84 at less than 10% discordance) in the sample gave an age of 16.2 ± 0.4 Ma (2σ). This grain is probably sourced from igneous rocks (volcanic-volcaniclastic?) of Miocene age, the like of which is unknown in the Arabian Gulf area. The sample shows the widest range of detrital zircon ages seen. It has two other young zircon grains at *c.*38 and 81 Ma. It also has a small number of Mesozoic grains with ages of 110, 133, 160 and 173 Ma. One grain of upper Palaeozoic age was recorded (ca 242 Ma, and two grains of lower Palaeozoic age (c. 458 and 493 Ma). The largest concentration of ages is between 572 and 699 Ma (36 grains), with lesser younger Neoproterozoic zircons between 528 and 562 Ma and older. A small but distinctive peak of early Neoproterozoic to Mesoproterozoic zircons at *c.* 986 (5 grains) is also seen. Five Palaeoproterozoic grains (1778, 2035, 2049, 2276, 2490 Ma) and one Neoarchean grain (2608 Ma) were recorded.

Sample UAE_7013 (70 concordant out of 78 analyses) has very similar detrital zircon age characteristics to UAE_7007 (Fig. 10). The youngest grain was dated at 36 ± 1 Ma (2σ), similar in age to the second-youngest grain in sample UAE_7007, suggesting that a Palaeocene igneous event of this age may be fairly widespread. The sample shows a more restricted range of Neo- to Mesoproterozoic zircons, but with similar peaks, suggesting that the age characteristics of the source areas of both samples were similar. However, the Neoproterozoic zircon population of sample UAE_7013 is distinctly bimodal, with major peak maxima at *c.* 615 (19 grains) and 784 Ma (12 grains). Both samples contain a similar minor component of older detritus, though with single zircon peaks at slightly different ages through the Mesoproterozoic to the Achaean. Sample UAE7013 has a single concordant Neoarchaean grain at 2826 Ma, being the oldest concordant zircon in the two samples, along with a discordant grain indicating a minimum age of >3330 Ma.

Quaternary Hili Formation (UAE_7026)

The U–Pb zircon data for a sample of fluvial sandstone from the Hili Formation are mostly concordant with 96 out of 101 analyses being within 10% of concordance. The two youngest concordant grains are dated at 39 ± 1 and 49 ± 1 Ma; other Phanerozoic grains are dated at *c.* 101 and 321 Ma. The most significant population spreads from 529 to 708 Ma (52 analyses) and features a peak at *c.* 630 Ma; a smaller population spreads from 750 to 1100 Ma (29 analyses). Two minor Palaeoproterozoic populations occur between 1873 and 2063 Ma (5 grains) and 2464 to 2495 Ma (4 grains), and two grains are Neoarchaean in age (2722 and 2727 Ma). The population is very similar to the other Quaternary samples, particularly UAE_7019

Quaternary Ghayathi Formation (UAE_7019)

Detrital zircons from a sample of dune cross-bedded aeolianite with a carbonate to quartz ratio of ~50:50 gave a similar age distribution to the Madinat Zayed Formation. The youngest grain recorded of 84 concordant grains (>90%; out of a total of 88 grains measured) was Palaeocene in age (36 ± 1 Ma), reinforcing evidence of an igneous event in the source area at that time. The sample contains a number of Mesozoic grains; two groups in the Cretaceous (c. 103 Ma) and Jurassic (ca 170 to 183 Ma), and one lower Palaeozoic grain (c. 456 Ma). The main age peak of zircons is seen in the Late Neoproterozoic between 607 and 654 Ma (22 grains). There is a consistently high input of older Neoproterozoic detritus with ages distributed between 673 to 893 Ma (29 grains). A minor peak of Late Mesoproterozoic zircons between 974 and 1128 Ma (9 grains) is also apparent. A small number of Palaeoproterozoic zircons are recorded (c. 1854, 1989 and 2327 Ma), along with quite a high number of Neoarchean zircons at *c.* 2514, 2518, 2519, 2548, 2602, 2641, 2653, 2712 and 2934 Ma (total of 9 grains) with one discordant grain indicating a possible earlier history with a minimum age of *c.* 3.5 Ga.

Modern sand dune (UAE_6145)

A sample of fine- to coarse-grained, poorly sorted, texturally and compositionally immature, calcareous quartzose aeolian sand comprising approximately 10 to 15% carbonate grains was analysed. Of the 91 zircon grains analysed 84 were concordant within 10%. The

youngest concordant grains were dated at ~1690 Ma (2 grains).The general age distribution is very similar to the Madinat Zayed Formation in particular. The sample contains a few (4) Palaeozoic grains, but the major peak is between *c.* 583 and 645 Ma, with 35 grains. A second, smaller but broader older Neoproterozoic peak between *c.* 720 and 875 Ma is also apparent, along with a minor number of Mesoproterozoic analyses between *c.* 1008 and 1044 Ma (3 grains). A few Palaeoproterozoic to Neoarchean grains are also present and one Mesoarchean grain dated at *c.* 2917 Ma.

6. Sediment Provenance.

The heavy mineral composition of the deposits preserved in the UAE can be used to identify distinct provenance fingerprints. The data reflect varying degrees of both mixing and recycling of older sediments from the underlying Miocene sediments (Shuwaihat and Baynunah formations), as well as inputs from the Gulf, the Hajar Mountains and the Arabian Shield.

6.1 Miocene sediments.

There is no distinguishable variation in heavy mineral component between the Baynunah and Shuwaihat formations suggesting they have the same provenance. The heavy mineral characteristics (low CZi and RZi) and the sedimentology of the deposits (Bristow & Hill 1998; Friend 1999; Farrant *et al.* 2012) suggest the bulk of the sediments were deposited by fluvial systems draining the Arabian shield. The Baynunah Formation in particular was deposited by a major fluvial system draining a quartz-rich hinterland to the NW. A second albeit minor component, defined by a distinct heavy mineral signature characterised by increased Mg (Fig. 9a) and Cr (Fig. 9b), can be identified. The location of this minor component is restricted to the most easterly outcrop of the Baynunah Formation SE of Abu Dhabi (Fig. 3). The increased Cr and Mg is diagnostic of a principally mafic source. This suggests that the eastern part of the Baynunah fluvial system drains the eastern flank of the Hajar Mountains, as a tributary to the main axial drainage. The detrital zircon dating indicates that the ultimate source of the Miocene sandstone units are the Neoproterozoic rocks of the Arabian Shield along with Palaeoproterozoic to Archaean basement remnants. In particular, the Shuwaihat Formation shows almost no post-Cambrian zircon sources. Significantly, the youngest detrital zircon grain in the Baynunah Formation constrains its maximum depositional age to *c.* 8 Ma, in line with other evidence of its age (Farrant *et al.* 2012).

6.2 Quaternary sediments

Each of the Quaternary formations sampled have a unique or semi-unique heavy mineral signature. The most distinctive is that of the Ghayathi Formation. The siliciclastic component of these carbonate rich palaeodune sandstones have heavy mineral signatures (CZi >35 and LSM dominated by calcic-amphibole and clinopyroxene with little orthopyroxene) significantly different from the Miocene, Madinat Zayed and Hili formation sediments. It is clear from both the mineralogy and geochemistry that the sediment source is profoundly different to either that of the Arabian Shield or Hajar Mountains. The Ghayathi Formation heavy mineral signature is most similar to sediments derived from the Tigris and Karun river systems at the head of the Arabian Gulf (Al-Juboury *et al.* 2009). A similar heavy mineral

composition was reported by Garzanti *et al.* (2013) for coastal sediments and beach deposits along the Gulf coast. The majority of the siliciclastic sediments in the Gulf are derived from material transported via the Tigris-Euphrates-Karun system. The marine carbonate composition of the Ghayathi Formation and the proximity of the outcrop to the coastline of the Arabian Gulf (Fig. 1) strongly suggests the palaeodunes are associated with the deflation of exposed unconsolidated sediments in the Gulf probably during periods of lower relative sea-level. The sediments were then blown onshore by the strong northwesterly Shamal winds. Dating suggests most of these dunes were emplaced and cemented at the onset of the Early Holocene humid period (Farrant *et al.* 2015). Some of the variation in the heavy mineral signature of the Ghayathi Formation can be explained by the admixture of sediments from the underlying Miocene bedrock as the dunes migrated inland. The RZI-CZi plot (Fig. 7) shows the Ghayathi Formation plots on a mixing trend with the Miocene sediments, with some of the samples further inland having lower CZi values. The raised marine Fuwayrit Formation sediments have a very similar heavy mineral signature to that of the Ghayathi Formation. The degree of heavy mineral variation is likely to be associated with preferential hydraulic sorting of the heavy minerals during deposition.

The detrital zircon signature of the Ghayathi Formation has a very similar age spectrum to the Miocene siliciclastics, and the Baynunah Formation in particular (Fig. 10), which shows a similarly strong Precambrian Arabian Shield signature with minor Phanerozoic input. This suggests some Arabian Shield inputs into the Gulf, possibly via the Wadi al-Batin fossil alluvial fan in Kuwait or from aeolian transport. The robust nature of the detrital zircons, coupled with a relative lack of younger sources of zircon elsewhere in the region compromises the use of detrital U–Pb geochronology as a tracer of sand.

The fluvial sediments of the Hili Formation are also distinct from the other units, having the largest concentration of orthopyroxene (Fig. 4 and 6a), and a LSMG and USMG biased towards a ferromagnesian-chromium facies. This and regional mapping (Farrant *et al.* 2012) strongly suggests that the Hili Formation is derived from the Hajar Mountains. The uplift and subsequent erosion of the Oman-UAE ophiolite is likely to have been a continued source of sediment to alluvial fan deposits since the early Neogene. The influence of the Hajar Mountains input extends as far west as Abu Dhabi. In terms of detrital zircon ages, the Hili Formation signature is almost identical to the Miocene Shuwaihat Formation, showing a predominance of second-phase derivation from Arabian Shield sources and very minor Mesozoic rock sources for its zircon populations.

In the northern Emirates, the Quaternary alluvial fans are sourced not from the ophiolite but the carbonate dominated Ruus al Jibal Mountains. Here, the fans are dominated by limestone clasts with a very minor siliciclastic component. The heavy mineral component of these fans is mineralogical similar to the source signature associated with the Ghayathi Formation (Arabian Gulf) with a near identical USM (Fig. 6b) and USMG (Fig. 6d). This suggests that much of the siliciclastic input into these alluvial deposits is derived not from the fan hinterland, but from reworked aeolian sedimentation blown onshore during periods of relative aridity and low sea-level by the northwesterly Shamal winds. A shift in the iron concentration in Fig. 6c could indicate a potentially minor shift in sediment source possibly

associated with the development of the limestone fans from the Mesozoic platform carbonates to the north east.

South and west of Abu Dhabi, the palaeodune sandstones of the Madinat Zayed Formation are not defined by a single heavy mineral signature (Fig. 6b and 6d). Two distinct clusters can be identified: the first mimics the signature associated with the bulk of the Miocene sediments, whilst the second population is more biased towards Cr/Cr-spinel. This same split is observed in the CZi:RZi plot (Fig. 7). The USM assemblage (Fig. 6a) is clinopyroxene/amphibole dominant and the associated LSMG (Fig. 6c) shows a very discrete population which is nearly identical to the predominant Miocene signature. It is apparent that most of the Madinat Zayed Formation is likely to be derived from the reworking of the Shuwaihat and Baynunah formations which forms the substrate over which the dunes have migrated, rather than being sourced from the Gulf or the Hajar Mountains. The exception is the component of the Madinat Zayed Formation with higher Cr concentrations which are located at the eastern margins of the outcrop. These samples probably represent mixing with ophiolitic sediments derived from the Hajar Mountains. In this regard, they are similar to the Miocene sediments with a distinct catchment divide in the area SE of Abu Dhabi. Detrital zircon spectra from two samples of the Madinat Zayed Formation are almost identical to each other and with that of the Miocene Baynunah Formation, showing strong second-phase Arabian Shield input and multiple Phanerozoic age-sources.

In the far west, the Sabkha Mati Formation exhibits a similar heavy mineral signature to Miocene sediments; however, there is insufficient evidence from the heavy mineral assemblage to categorically define this formation as either primary Arabian Shield detritus or reworked Miocene sediments. The presence of large igneous clasts within the formation suggests that the sands are likely to be derived from reworking of the Hofuf Formation which occurs a short distance to the west.

6.3 Modern dune sands

The LSM, USM and USMG all show degrees of overlap with one or more defined sediment source signatures, suggesting the modern dune sands are composed of a mix of sediments derived from reworking of Miocene sediments, inputs from the Hajar Mountains (via modern and Quaternary fluvial systems) and blown onshore from the Gulf. However, the LSMG (Fig. 6c) shows a population of dune sands which appear unique with no comparable source signature. This Fe-depleted, Ca/Mg rich population is associated with a large contribution of detrital dolomite (Fig. 11), which includes a minor component of detrital serpentine with possible chrysotile veins. The location of these dolomitic dune sands in close proximity to outcrops of the strongly dolomitised Miocene Barzaman Formation (Lacinska *et al.* 2014) suggests they are the source of the sediment. Strong deflation led to the incorporating of detrital dolomite and related ophiolitic detritus into the dunes downwind of the outcrop.

The established source signatures (Arabian Shield, Arabian Gulf, Hajar Mountains), along with distinctive local inputs such as the Barzaman Formation can be applied to determine the provenance for the Rub' al-Khali desert sands of the UAE. The LSMG (Fig. 6c) and USMG

649 (Fig. 6d) are used because the source signatures are better defined, a greater number of
650 samples were analysed using this method and are directly representative of the bulk heavy-
651 mineral composition.

652 Broad source signatures are created based on the population clusters previously established
653 (Fig. 12a & b). For both figures there is a degree of overlap between the source signatures,
654 further discrimination is achieved through transects formed between intersects of source
655 signatures. The location and associated source signatures are shown in Fig. 13. The solid
656 markers represent an USMG and LSMG component with the same source signature. Where
657 signatures are varied; the left segment represents the USMG component and the right
658 segment the LSMG component. The estimated degree of mixing between proximal sources
659 is based upon the framework in Fig. 12.

660 The heavy mineral data shows there is a clear change in sand composition to the south and
661 east (Fig. 13). Modern carbonate dune sands near the coast have a clear Gulf component. As
662 the dunes migrate inland, this Gulf component decreases as increasing amounts of
663 siliciclastic sand derived from the deflation of Miocene sandstones is incorporated. East of
664 Abu Dhabi, the same process occurs, but here the deflation of the Miocene Barzaman
665 Formation and the Hili Formation liberates sand with a distinct Hajar Mountains signature.
666 The sample of modern dune sand that underwent detrital zircon U–Pb analysis has an age-
667 probability spectrum that mirrors that of the Quaternary Madinat Zayed Formation and, in
668 turn, the Miocene Baynunah Formation. This indicates the zircon populations from the
669 Arabian Shield and multiple Phanerozoic sources have undergone multiple reworking, with
670 few additional inputs from local sources.

671 The volume of dune sand liberated from the deflation of the Miocene and Quaternary
672 sandstones along the Arabian Gulf coast is considerable. The Miocene sandstones are up to
673 80 m thick and extend 200 km from Abu Dhabi to Sabkha Mati, and once extended,
674 probably continuously, at least as far north as the island of Delma, 50 km offshore. It is thus
675 likely that at least 500 km^3 of sediment has been deflated and blown inland by the
676 predominant northwesterly Shamal winds, representing a significant proportion of the
677 present Rub' al-Khali dune-field. The Miocene sandstones in turn probably originated in part
678 from the erosion of the thick Palaeozoic siliciclastic successions that surround the
679 Neoproterozoic shield in Saudi Arabia. Moreover, these Miocene sediments have been
680 partially recycled though at least one set of Quaternary palaeodunes (the Madinat Zayed
681 Formation) prior to being incorporated into the modern Rub' al-Khali dunes. The component
682 of sand derived from the Hajar Mountains is relatively small and restricted to the northern
683 Emirates east of Abu Dhabi. Localised deflation of the Barzaman Formation in interdune
684 hollows contributes a small, but significant supply of sediment to the dunes in the eastern
685 Emirates.

686 **Conclusions**

687 Analysis of the heavy mineral composition of sediments in the UAE reveals much about the
688 geological history of the region. Combined with data from geological mapping (Farrant *et al.*

689 2012), a more refined picture of sediment provenance and movement can be determined
690 (Fig. 14).

691 Garzanti *et al.* 2013 suggest that most of the sand in the Rub' al-Khali sand seas is ultimately
692 derived from the Arabian Shield, and transported in part via the Nafud, Dahna and western
693 Jafurah sand corridors, with a small component derived from the Gulf. Whilst it is true that
694 most of the sand in the UAE has an Arabian shield origin, this only part of a complex history
695 and it is clear the sand has been recycled multiple times. The data from the UAE suggests
696 that sand in the northern part of the Rub' al-Khali sand-sea is derived not by the long-
697 distance transport of aeolian sand from northern Arabia, but locally derived sand from the
698 deflation of Miocene fluvial sandstones and younger Quaternary deposits along the upwind
699 margin of the dune-field.

700 A smaller component of sediment is derived from the Arabian Gulf. The carbonate-rich
701 palaeodunes (Ghayathi Formation) and raised marine deposits (Fuwayrit Formation) along
702 the Gulf coast testify to the supply of sediment from the Gulf during periods of lower sea-
703 level. The heavy mineral composition suggests that the Tigris–Euphrates–Karun river system
704 is the ultimate source of this sand (Garzanti *et al.* 2013). Assuming eustatic models of sea-
705 level are correct (Lambeck *et al.* 1996; Teller *et al.* 2000), fluvio-deltaic sediments deposited
706 by this system would have prograded southeastwards along the axis of the Gulf foreland
707 basin during Pleistocene lowstands. Some of this material was subsequently blown onshore
708 by strong northwesterly Shamal winds during arid periods. Notwithstanding the above,
709 however, even the carbonate dunes of the Ghayathi Formation show considerable evidence
710 of a re-worked Arabian Shield parentage in their detrital zircon age spectrum.

711 A third component of sediment is derived from the Hajar Mountains. Geological mapping
712 and the heavy mineral data suggests that the Hajar Mountains were contributing sediment
713 as far west as Abu Dhabi, both in the Miocene and the Quaternary. The Hili Formation and
714 to a lesser extent the Madinat Zayed Formation are directly associated with detritus derived
715 from the Hajar Mountains. However, due to the prevailing northwesterly wind direction, the
716 sediment from this source is restricted to a relatively small area of the northern Emirates.
717 Some of the aeolian sand that migrates onto the alluvial fans during arid periods is reworked
718 into the fluvial sandstones in subsequent wet periods. It is noteworthy that the Hajar
719 Mountain component is poorly reflected in the detrital zircon age record because most of
720 the rocks which form the mountains are very zircon-poor (e.g. Roberts *et al.* 2016).

721 Based on these interpretations an estimated 50-60% of the Rub' al-Khali desert sands of the
722 UAE are derived ultimately from the Arabian Shield via the deflation of Miocene sandstones
723 and the erosion of Quaternary deposits derived therefrom. The Arabian Gulf and Hajar
724 Mountain sources each contribute another 15-20% .Some of the Hajar heavy mineral
725 signature (probably less than 5%) is recycled via the Miocene Barzaman Formation. The
726 effect of this source-mixing is clearly seen. To the SE, an increasing proportion of the dune
727 sand is derived from the Hajar Mountains as the dunes migrate southeastwards over
728 Miocene and Quaternary ophiolite rich alluvial fan deposits (Hili and Barzaman formations).
729 To the south, the Arabian Shield component increases as the Gulf-derived sediments

become increasingly diluted as the dunes migrate over weak, friable, rapidly deflating Miocene and Quaternary sandstones.

This model of sediment supply is supported by the U–Pb age spectra which are typically characterised by a Neoproterozoic peak indicative of an Arabian Shield origin. The modern dune sands have a similar age spectrum to the Madinat Zayed Formation substrate which in turn has affinities with the Miocene siliciclastic deposits from which they are derived.

Acknowledgements

We thank the help and support of Saleh Al Mahmoodi, Khalid Al Hosani and Abdullah Gahnoog of the Department of Mineral and Energy Resources, Ministry of Energy, Abu Dhabi, for their support during the geological mapping of the UAE, and M. Horstwood and A. Wood for analytical assistance. Farrant, Mounteney, Roberts and Bide publish with the approval of the Executive Director of the British Geological Survey. This paper is dedicated to the memory of Robert Knox who sadly passed away during this research project.

References

Al-Juboury, A.I. & Al-Miamary, F.A. 2009. Geochemical variations in heavy minerals as provenance indications: application to the Tigris river sand, northern Iraq. *Journal of Mediterranean Earth Sciences*, *1*.

Al-Juboury, A.I., Ghazal, M.M, & McCann, T. 2009. Detrital chromian spinels from Miocene and Holocene sediments of northern Iraq: provenance implications. *Journal of Geosciences*, 54, 289–300.

Al-Saad, H., Nasir, S., Sadooni, F. & Alsharhan A.S. 2002: Stratigraphy and sedimentology of the Hofuf Formation in the State of Qatar in relation to the tectonic evolution of the East Arabian Block. *Neues Jahrbuch für Geologie und Paläontologie-Monatshefte*. 7, 426-448; Stuttgart.

Al-Safarjalani, A.M. 2004. Placer gold deposits in the Hofuf Formation, the eastern province of Saudi Arabia, research project Nr. 4022. *King Faisal University, Faculty of Agriculture, Department of Soil and Water, Al-Hofuf*, *101*.

Alsharhan, A. S., & Nairn A. E. M. 1997. *Sedimentary Basins and Petroleum Geology of the Middle East*, Elsevier, Amsterdam.

Andò, S., Garzanti, E., Padoan, M. & Limonta, M. 2012. Corrosion of heavy minerals during weathering and diagenesis: A catalogue for optical analysis. *Sedimentary Geology* 280, 165-178.

Aqrawi, A.A. & Evans, G. 1994. Sedimentation in the lakes and marshes (Ahwar) of the Tigris-Euphrates Delta, southern Mesopotamia. *Sedimentology*, 41, 755-776.

Bassis, A., Hinderer, M. & Meinhold, G. 2016. New insights into the provenance of Saudi Arabian Palaeozoic sandstones from heavy mineral analysis and single-grain geochemistry. *Sedimentary Geology*, 333, 100-114.

Bristow, C.S., & Hill, N. 1998. Dune morphology and palaeowinds from aeolian sandstones in the Miocene Shuwaihat Formation, Abu Dhabi, United Arab Emirates. *In*: Alsharhan A.S., Glennie K.W., Whittle G.L. & Kendall, C. G. StC. (eds) *Quaternary Deserts and Climatic Change.* Rotterdam, The Netherlands, Balkema, 553-564.

771 Dill, H.G., Botz, R., Berner, Z., Stüben, D., Nasir, S. & Al-Saad, H. 2005. Sedimentary facies,
772 mineralogy, and geochemistry of the sulphate-bearing Miocene Dam Formation in Qatar.
773 *Sedimentary Geology*, 174, 63-96.

774 Farrant, A.R. & Ellison, R.A. 2014. Sand, sea and sabkhas – the Quaternary story of the
775 desert and the Arabian Gulf coast. *In*: Thomas, R.J. & Ellison, R.A. (eds). *Geological evolution*
776 *of the United Arab Emirates. Over six hundred million years of Earth History*. Keyworth,
777 Nottingham: British Geological Survey, 219-262

778 Farrant, A.R., Duller, G.A., Parker, A.G., Roberts, H.M., Parton, A., Knox, R.W. & Bide, T.
779 2015. Developing a framework of Quaternary dune accumulation in the northern Rub'al-
780 Khali, Arabia. *Quaternary International*, *382*, 132-144.

781 Farrant, A.R., Ellison, R.A. Thomas, R.J. Pharaoh, T.C. Newell, A.J. Goodenough K.M., Lee, J.R.
782 & Knox, R.O.B. 2012. *The Geology and Geophysics of the United Arab Emirates. Volume 6:*
783 *Geology of the western and central United Arab Emirates*, British Geological Survey,
784 Keyworth, Nottingham.

785 Fedo, C.M., Sircombe, K.N. & Rainbird, R.H. 2003. Detrital zircon analysis of the sedimentary
786 record. *Reviews in Mineralogy and Geochemistry*, *53*1, 277-303.

787 Friend, P.F. 1999. Rivers of the Lower Baynunah Formation. Emirate of Abu Dhabi. United
788 Arab Emirates. In: Whybrow, P.J. & Hill, A.P. (eds). *Fossil vertebrates of Arabia: with*
789 *emphasis on the late Miocene faunas, geology, and palaeoenvironments of the Emirate of*
790 *Abu Dhabi, United Arab Emirates*. Yale University Press, Newhaven.

791 Garzanti, E., Al-Juboury, A.I., Zoleikhaei, Y., Vermeesch, P., Jotheri, J., Akkoca, D.B., Obaid,
792 A.K., Allen, M.B., Andó, S., Limonta, M. & Padoan, M. 2016. The Euphrates-Tigris-Karun river
793 system: Provenance, recycling and dispersal of quartz-poor foreland-basin sediments in arid
794 climate. *Earth-Science Reviews*, *162*, 107-128.

795 Garzanti, E., Andò, S., Vezzoli, G, & Dell'era, D. 2003. From rifted margins to foreland basins:
796 investigating provenance and sediment dispersal across desert Arabia (Oman, U.A.E.).
797 *Journal of Sedimentary Research*, 73, 572–588.

798 Garzanti, E., Vermeesch, P., Andò, S., Vezzoli, G., Valagussa, M., Allen, K., Kadi, K.A. & Al-
799 Juboury, A.I. 2013. Provenance and recycling of Arabian desert sand. *Earth-Science Reviews*,
800 *120*, 1-19.

801 Gehrels, G. 2011. Detrital Zircon U-Pb Geochronology: Current Methods and New
802 Opportunities. *In:* Busby, C. & Azor, A (eds), Tectonics of Sedimentary Basins: Recent
803 Advances John Wiley & Sons, Ltd, Chichester, UK. doi: 10.1002/9781444347166.ch2

804 Glennie, K.W. & Singhvi, A.K. 2002. Event stratigraphy, paleoenvironment and chronology of
805 SE Arabian deserts. *Quaternary Science Reviews*, 21, 853-869.

806 Goodenough, K.M., Thomas, R.J., Styles, M.T., Schofield, D.I. & MacLeod, C. 2014. Records of
807 ocean growth and destruction in the Oman – UAE ophiolite. *Elements,* 10, 105-110.

808 Horstwood, M.S., Košler, J., Gehrels, G., Jackson, S.E., McLean, N.M., Paton, C., Pearson, N.J.,
809 Sircombe, K., Sylvester, P., Vermeesch, P. & Bowring, J.F. 2016. Community-Derived
810 Standards for LA-ICP-MS U-(Th-) Pb Geochronology–Uncertainty Propagation, Age
811 Interpretation and Data Reporting. *Geostandards and Geoanalytical Research*, 40, 311-332.

812 Jacobs, J., Thomas, R. J., Ksienzyk, A. & Dunkl, I. 2015. Tracking the Oman Ophiolite to the
813 surface – new fission track and U-Th/He data from the Aswad and Khor Fakkan blocks,
814 United Arab Emirates**.** *Tectonophysics,* **644-645**, 68-80.
815 http://dx.doi.org/10.1016/j.tecto.2014.12.018

816 Kumar-Jain, Y. & Bhandare, S. K. 2011. Min max normalization based data perturbation
817 method for privacy protection. *International Journal of Computer and Communication*
818 *Technology* 2, 45–50.

819 Lacinska, A.M., Styles, M.T. & Farrant, A.R. 2014. Near-surface diagenesis of ophiolite-
820 derived conglomerates of the Barzaman Formation, United Arab Emirates: a natural
821 analogue for permanent CO2 sequestration via mineral carbonation of ultramafic rocks.
822 *Geological Society, London, Special Publications*, *392*1, 343-360.

823 Lambeck, K. 1996. Shoreline reconstructions for the Persian Gulf since the last glacial
824 maximum. *Earth and Planetary Science Letters*, *142*1-2, 43-57.

825 Mercolli, I., Briner, A.P., Frei, R., Schönberg, R., Nägler, T.F., Kramers, J. & Peters, T. 2006.
826 Lithostratigraphy and geochronology of the Neoproterozoic crystalline basement of Salalah,
827 Dhofar, Sultanate of Oman. *Precambrian Research*, *145* 3, 182-206.

828 Morton, A.C. & Hallsworth, C.R. 1994. Identifying provenance-specific features of detrital
829 heavy mineral assemblages in sandstones. *Sedimentary Geology*, 90, 241–256.

830 Morton, A.C. 1985 Heavy Minerals in Provenance Studies. *In:* Zuffa, G.G. (Ed) *Provenance of*
831 *Arenites*. Springer Netherlands, Dordrecht, 249-277.

832 Mounteney, I. Burton, A.K., Farrant, A.R. Watts, M.J. Kemp, S.J. & Cook, J.M. 2017. Heavy
833 mineral analysis by ICP-AES for rapid sediment provenancing. In press.

834 Mouthereau, F., Lacombe, O. & Vergés, J., 2012. Building the Zagros collisional orogen:
835 timing, strain distribution and the dynamics of Arabia/Eurasia plate convergence.
836 *Tectonophysics*, 532, 27-60.

837 Newell, A.J, Goodenough, K.M., Farrant, A.R, Ellison, R.A & Thomas, R.J. 2012. Geology of
838 the Gheweifat and As Sila 1:100 000 map sheet, United Arab Emirates. Keyworth,
839 Nottingham: British Geological Survey.

840 Newell, A.J., & Farrant, A.R. 2014. Final retreat of the Neothys – the Neogene. *In:* Thomas,
841 R.J. & Ellison, R.A. (eds). *Geological evolution of the United Arab Emirates. Over six hundred*
842 *million years of Earth History*. Keyworth, Nottingham: British Geological Survey, 189-217.

843 Parton, A., Farrant, A.R., Leng, M.J., Telfer, M.W., Groucutt, H.S., Petraglia, M.D. & Parker,
844 A.G. 2015. Alluvial fan records from southeast Arabia reveal multiple windows for human
845 dispersal. *Geology*, 43, 295-298.

846 Philip, G. 1968. Mineralogy of recent sediments of Tigris and Euphrates rivers and some of
847 the older detrital deposits. *Journal of Sedimentary Research*, 38, 35-44.

848 Powers, R.W., Ramirez, L.F., Redmond, C.D. and Elberg Jr, E.L., 1966. *Geology of the Arabian*
849 *Peninsula—Sedimentary Geology of Saudi Arabia.* United States Geological Survey
850 Professional Paper, 560-D. U.S. Government Printing Press, Washington, DC.

Roberts, N.M.W, Parrish, R.R., Horstwood, M.S. & Brewer, T.S. 2011. The 1.23 Ga Fjellhovdane rhyolite, Grøssæ-Totak; a new age within the Telemark supracrustals, southern Norway. *Norwegian Journal of Geology*, 91, 239-246.

Roberts, N.M.W, Thomas, R.J. & Jacobs, J., 2016. Geochronological constraints on the metamorphic sole of the Semail ophiolite in the United Arab Emirates. *Geoscience Frontiers*, 7, 609-619.

Searle, M.P., Cherry, A.G., Ali, M.Y. & Cooper, D.J., 2014. Tectonics of the Musandam Peninsula and northern Oman Mountains: From ophiolite obduction to continental collision. *GeoArabia,* 19, 135-174.

Skoček, V. & Saadallah, A.A. 1972. Grain-size distribution, carbonate content and heavy minerals in eolian sands, southern desert, Iraq. *Sedimentary Geology*, 81, 29-46.

Spencer, C.J., Kirkland, C.L. & Taylor, R.J. 2016. Strategies towards statistically robust interpretations of in situ U–Pb zircon geochronology. *Geoscience Frontiers*, 7, 581-589.

Stern, R.J. & Johnson, P. 2010. Continental lithosphere of the Arabian Plate: A geologic, petrologic and geophysical synthesis. *Earth Science Reviews,* 101**,** 29-67.

Stern, R.J. 1994. Arc assembly and continental collision in the Neoproterozoic East African orogeny—implications for the consolidation of Gondwana. *Annual Review of Earth and Planetary Sciences* 22, 319–351.

Stern, R.J., Ali, K.A., Liégeois, J.P., Johnson, P.R., Kozdroj, W. & Kattan F.H. 2010. Distribution and significance of pre-Neoproterozoic zircons in juvenile Neoproterozoic igneous rocks of the Arabian-Nubian Shield. *American Journal of Science*, 310, 791-811.

Styles, M.T, Ellison, R.A, Arkley, S., Crowley, Q.G., Farrant, A.R, Goodenough, K.M., McKervey, J., Pharaoh, T., Phillips, E. & Schofield, D.I. 2006. The Geology and Geophysics of the United Arab Emirates: Volume 2, Geology. British Geological Survey, Keyworth, Nottingham.

Teller, J.T., Glennie, K.W., Lancaster, N. & Singhvi, A.K. 2000. Calcareous dunes of the United Arab Emirates and Noah's Flood: the postglacial reflooding of the Persian (Arabian) Gulf. *Quaternary International*, 68, 297-308.

Thomas, R J, & Ellison, R A. (eds) 2014. *Geological evolution of the United Arab Emirates. Over six hundred million years of Earth History*. Keyworth, Nottingham: British Geological Survey, 287

Thomas, R J., Ellison, R A., Goodenough, K.M., Roberts, N.M.W. & Allen, P.A. 2015. Salt domes of the UAE and Oman: probing eastern Arabia. *Precambrian Research,* **256**, 1–16.

Thomas, R.J., Roberts, N.M.W, Jacobs, J., Bushi, A.M., Horstwood, M.S. & Mruma, A. 2013. Structural and geochronological constraints on the evolution of the eastern margin of the Tanzania Craton in the Mpwapwa area, central Tanzania. *Precambrian Research*, 224, 671-689.

Vermeesch, P. 2012. On the visualisation of detrital age distributions. *Chemical Geology*, 312, 190-194.

890 Vermeesch, P., Fenton, C.R., Kober, F., Wiggs, G.F.S., Bristow, C.S. & Xu, S. 2010. Sand
891 residence times of one million years in the Namib Sand Sea from cosmogenic nuclides.
892 *Nature Geoscience*, *3*12, 862-865.

893 Whitehouse, M.J., Windley, B.F., Stoeser, D.B., Al-Khirbash, S., Ba-Bttat, M.A. & Haider, A.
894 2001. Precambrian basement character of Yemen and correlations with Saudi Arabia and
895 Somalia. *Precambrian Research*, *105*2, 357-369.

896 Whybrow, P.J. & Hill, A.P. (eds). 1999. *Fossil vertebrates of Arabia: with emphasis on the late*
897 *Miocene faunas, geology, and palaeoenvironments of the Emirate of Abu Dhabi, United Arab*
898 *Emirates*. Yale University Press, Newhaven.

899 Williams, A.H. & Walkden, G.M. 2002. Late Quaternary highstand deposits of the southern
900 Arabian Gulf: a record of sea-level and climate change. *Geological Society, London, Special*
901 *Publications*, *195*1, 371-386.

902 Wood, W.W., Bailey, R.M., Hampton, B.A., Kraemer, T.F., Lu, Z., Clark, D.W., James, R.H. & Al
903 Ramadan, K. 2012. Rapid late Pleistocene/Holocene uplift and coastal evolution of the
904 southern Arabian (Persian) Gulf. *Quaternary Research*, *77*2, 215-220.

905

906

907 **Tables**

908

Sample	Easting	Northing	Stratigraphic unit	Sample description
UAE_6145	301722	2611230	Recent dune sand	Modern dune sand
UAE_7019	184367	2626744	Ghayathi Fm	Cross-bedded aeolianite
UAE_7026	301793	2673600	Hili Fm	Beige fluvial (?) sandstone
UAE_7007	210753	2610218	Madinat Zayed Fm	Cross-bedded aeolianite
UAE_7013	229366	2612014	Madinat Zayed Fm	Greenish-grey fluvial (?) sandstone
UAE_7422	163465	2652754	Baynunah Fm	Rhizolithic red sandstone
UAE_6380	197903	2663069	Shuwaihat Fm	Red aeolian sand

909 **Table 1.** *Metadata for the seven U–Pb detrital zircon samples from the Miocene to recent*
910 *sediments (coordinates in UTM Zone 40)*

911

912 **Figures**

913

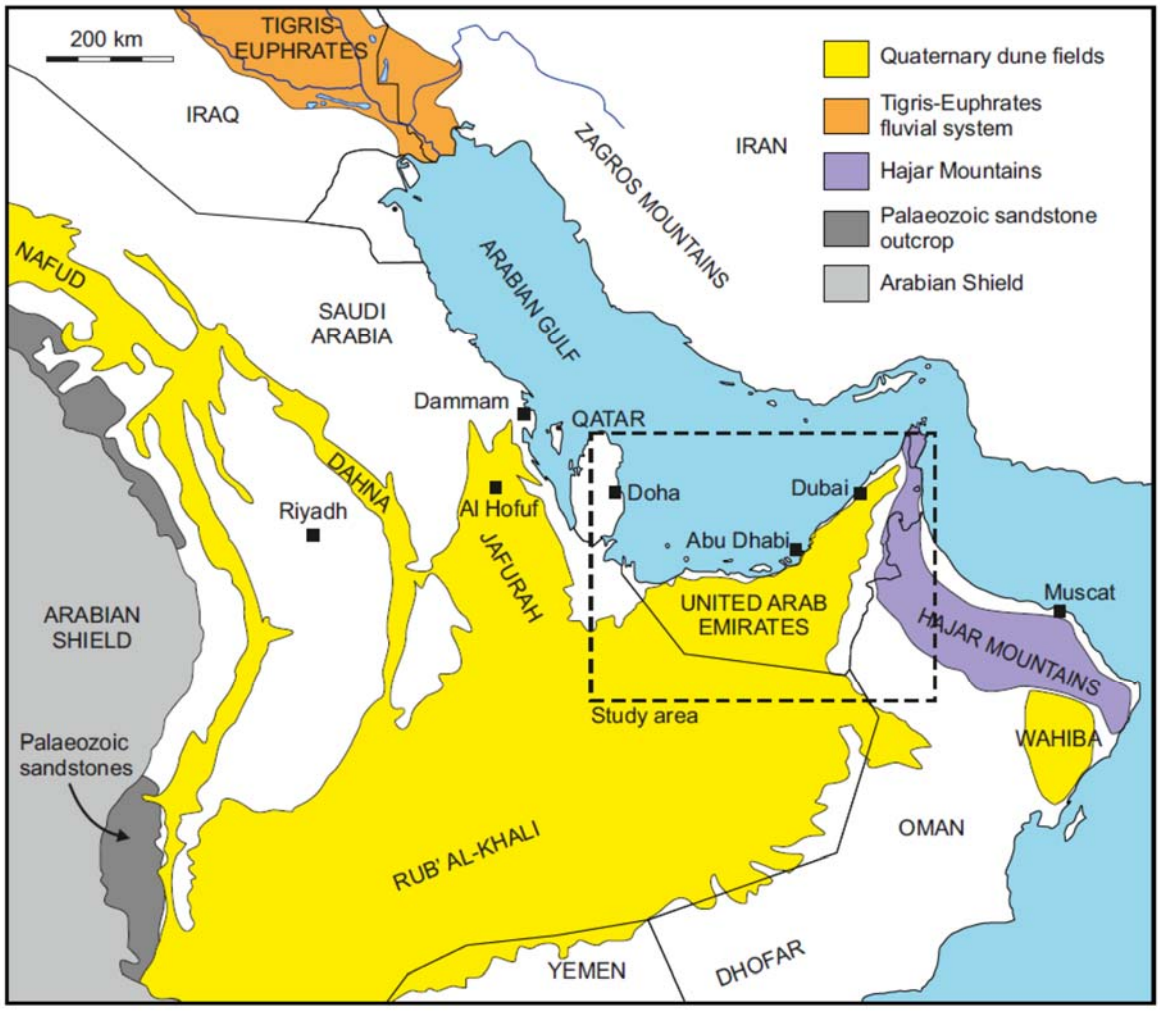

914

915 Fig. 1. Simplified geological map of Arabia showing main Quaternary dune fields.

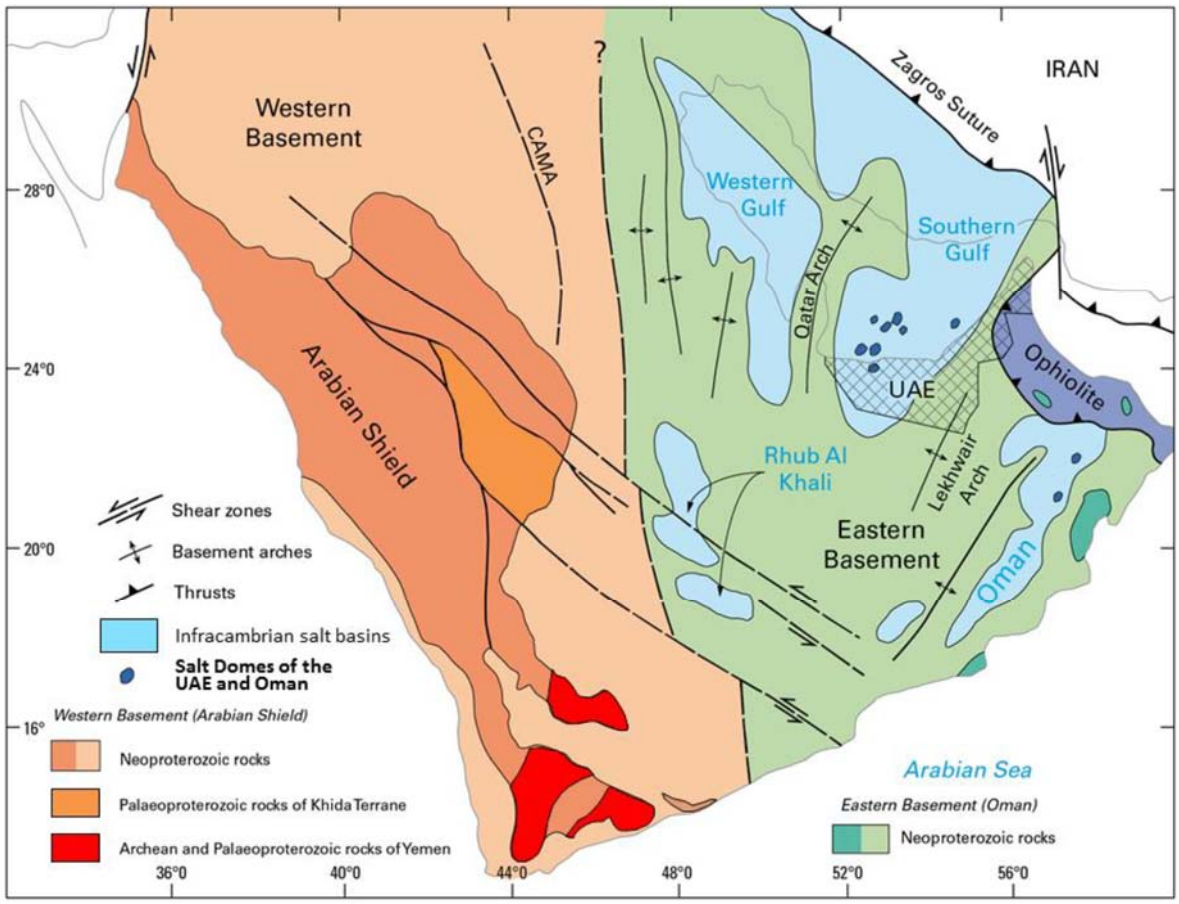

916

917 Fig. 2. Geological architecture of the Arabian Plate (modified after Stern & Johnson 2010, in
918 Thomas *et al.* 2015).

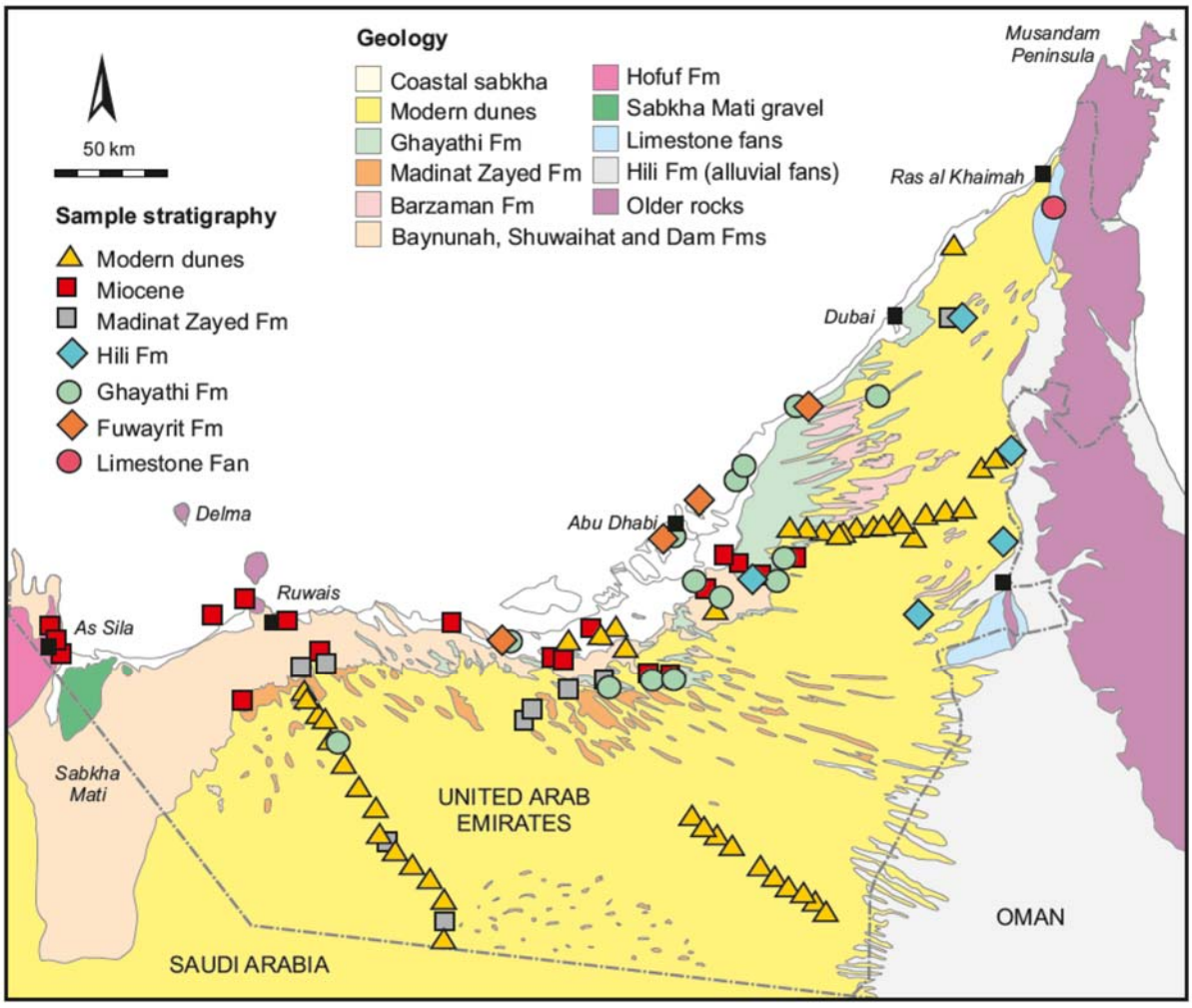

919

920 Fig. 3. Simplified geological map of the UAE based on Styles et al. (2006) and Farrant et al.
921 (2012). Heavy mineral sample locations are shown, grouped by stratigraphy.

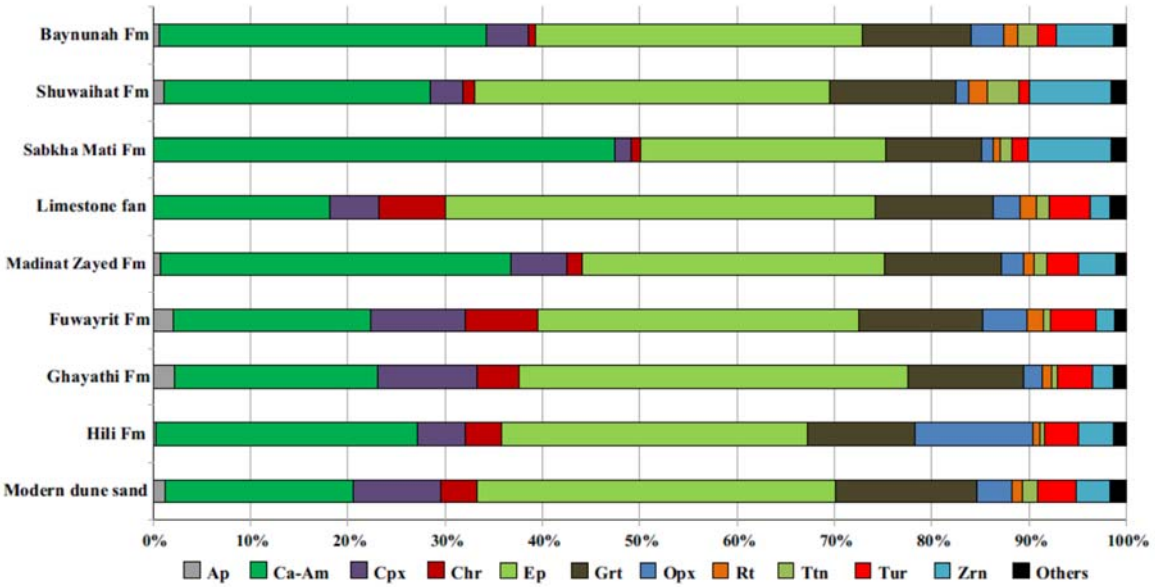

922

923 Fig. 4. Average detrital heavy-mineral assemblages for each geological unit sampled.

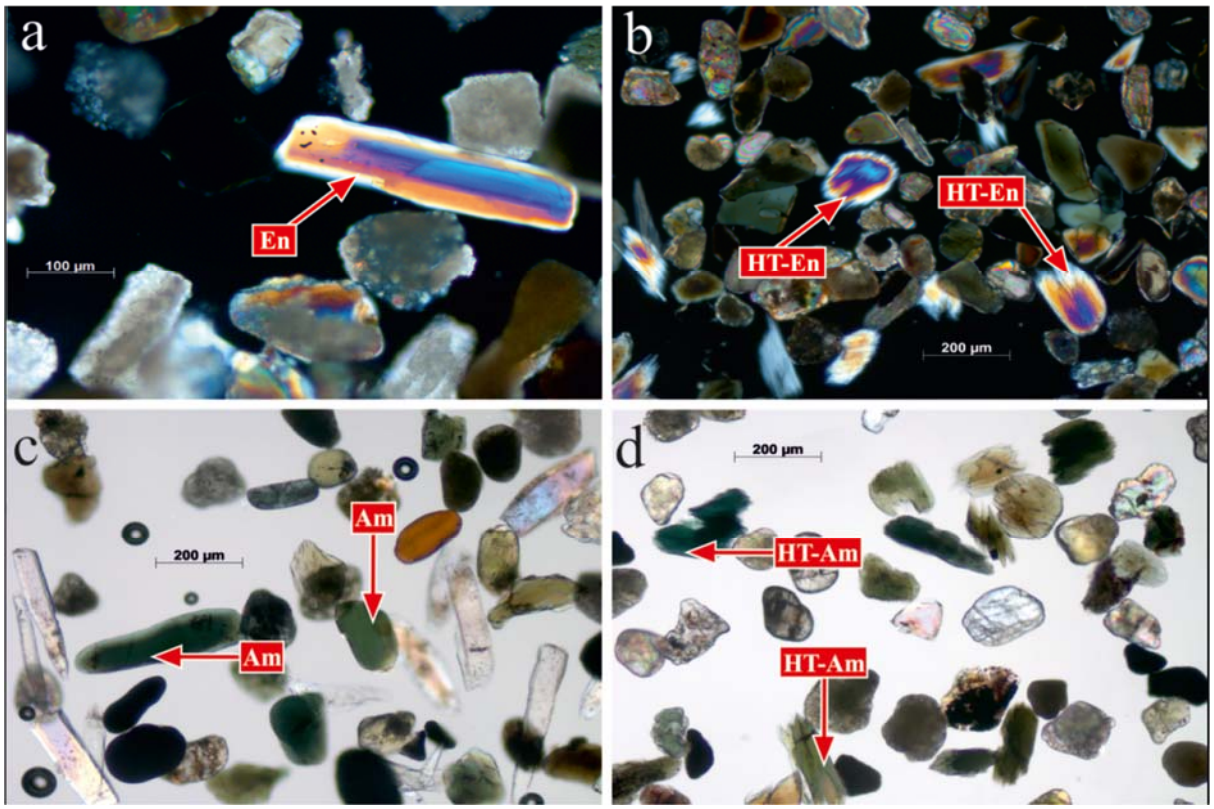

924

925 Fig. 5. Unaltered Enstatite (**a**) and unaltered amphibole (**c**); partial dissolution of enstatite
926 (**b**) and amphibole (**d**), displaying characteristic hacksaw terminations.

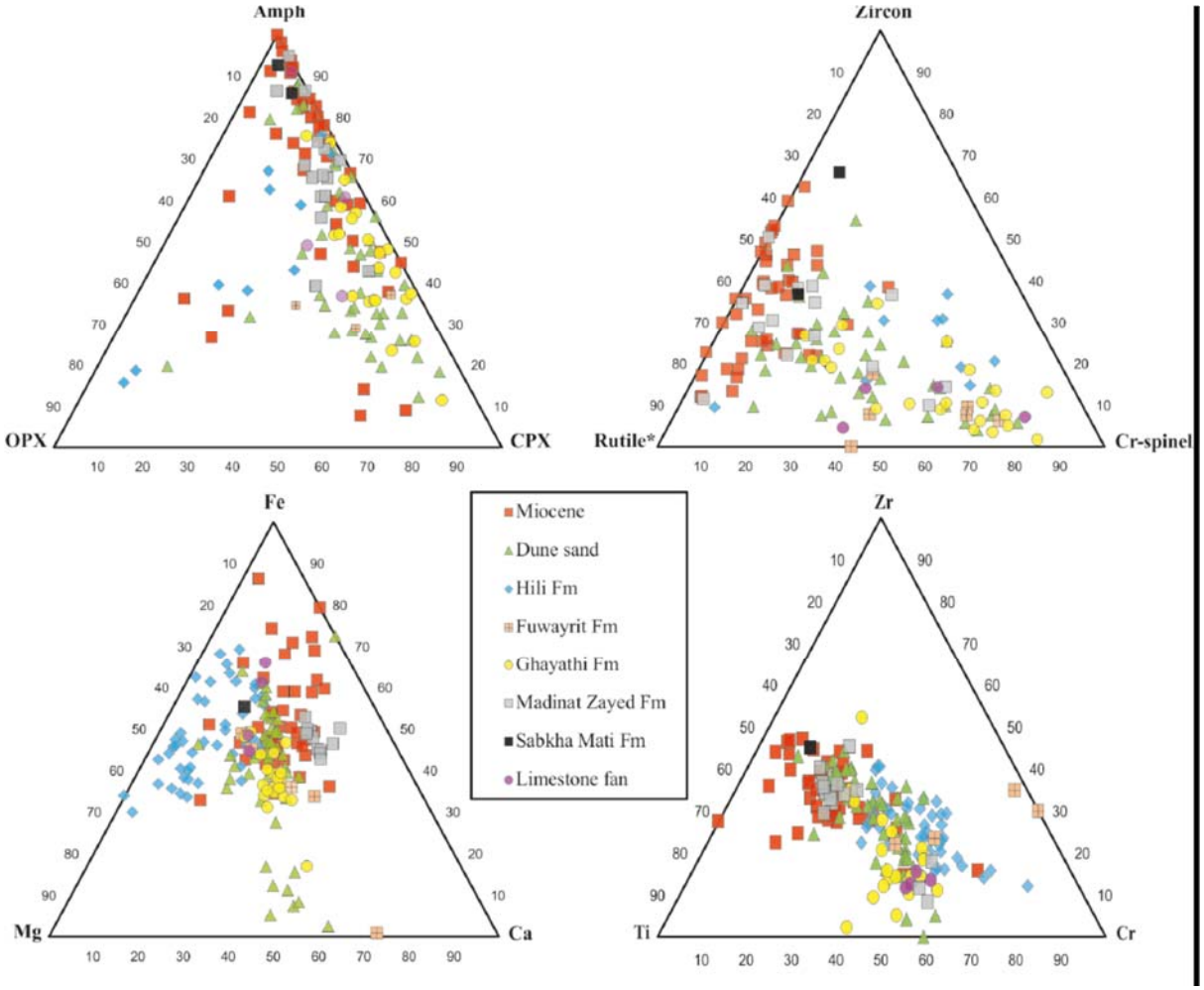

927

928 Fig. 6. Ternary plots showing (**a**) less-stable minerals (LSM), (**b**), ultra-stable minerals (USM),
929 (**c**) less-stable mineral geochemistry (LSMG) and (**d**), ultra-stable mineral geochemistry
930 (USMG).

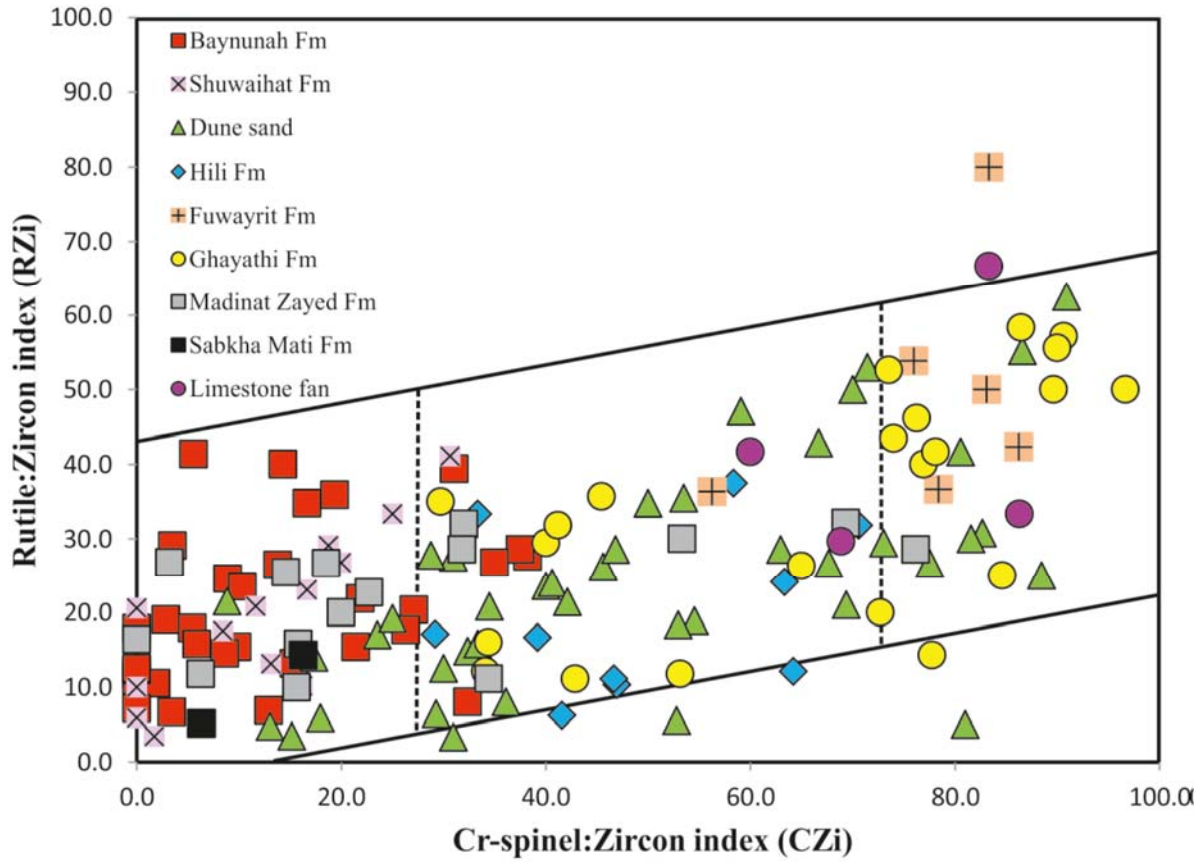

931

932 Fig. 7. Chrome-spinel:zircon index (CZi) and rutile:zircon index (RZi) mineral index
933 comparison chart showing the distribution of samples (grouped by lithological type) and the
934 mixing trend

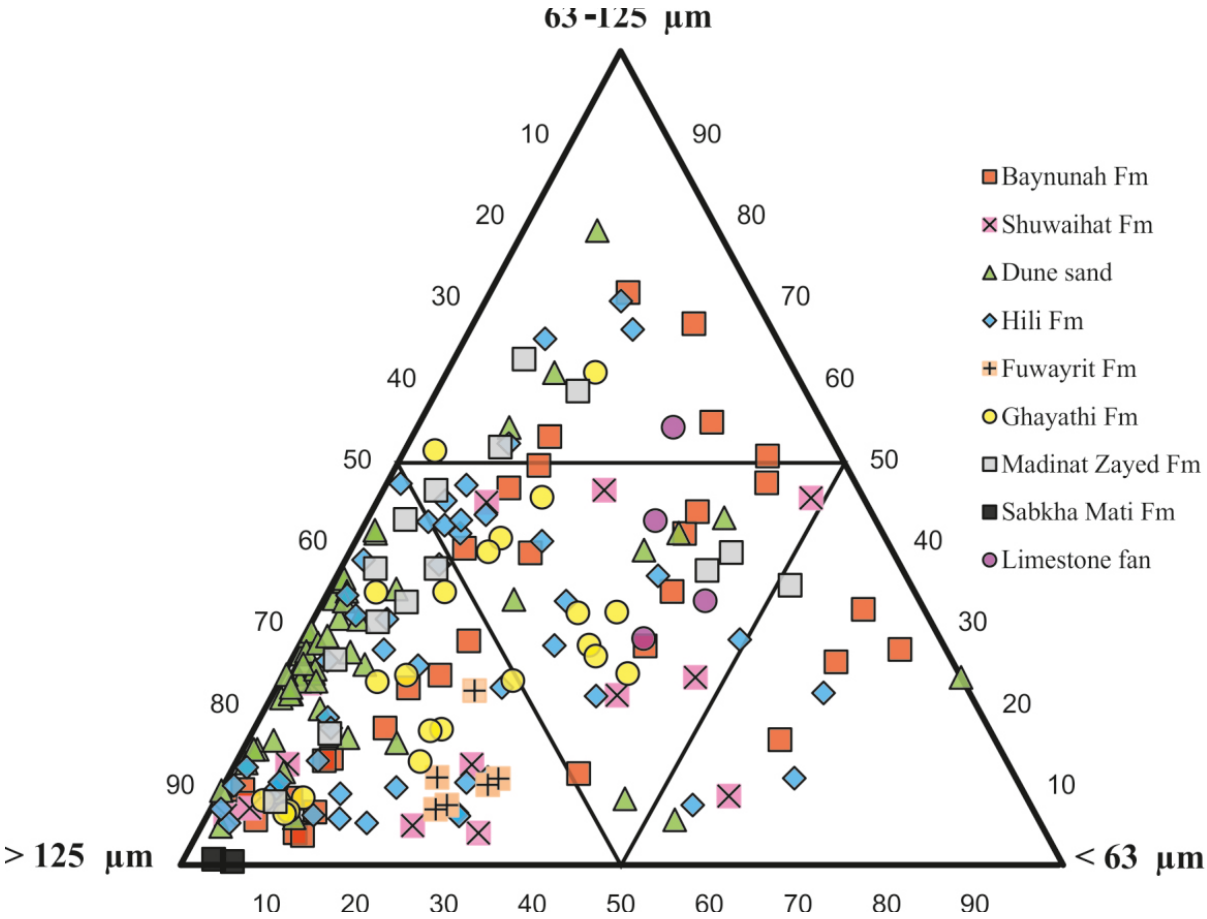

935

936 Fig. 8. Grain size distribution of: clay and silt sized particles (< 63 µm), fine-grained sand (63-
937 125 µm) and > medium-grained sand (> 125 µm).

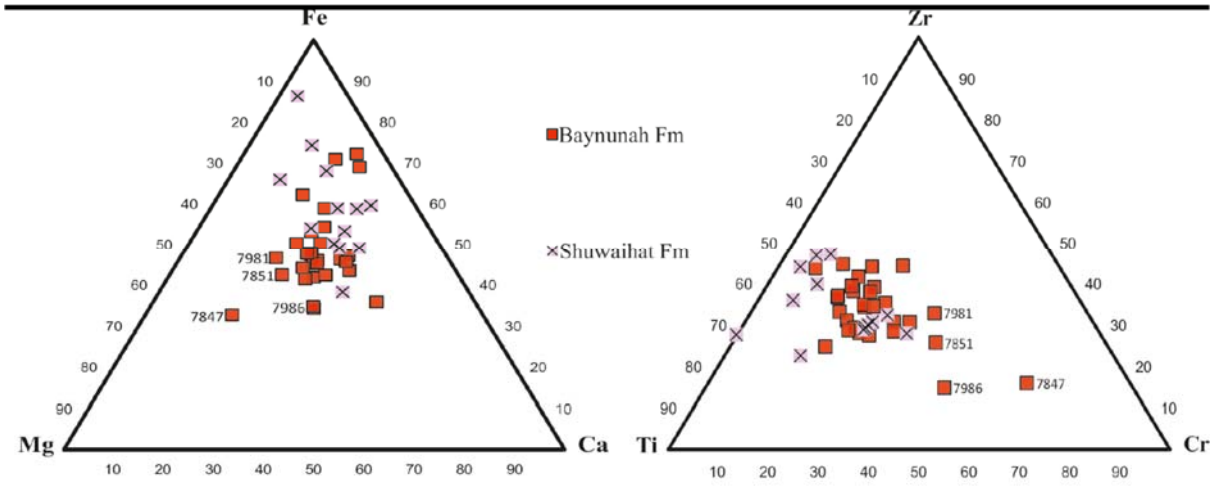

938

939 Fig. 9. (**a**) less-stable mineral geochemistry (LSMG) plot for Miocene sediments; (**b**) ultra-
940 stable mineral geochemistry (USMG) plot for Miocene sediments.

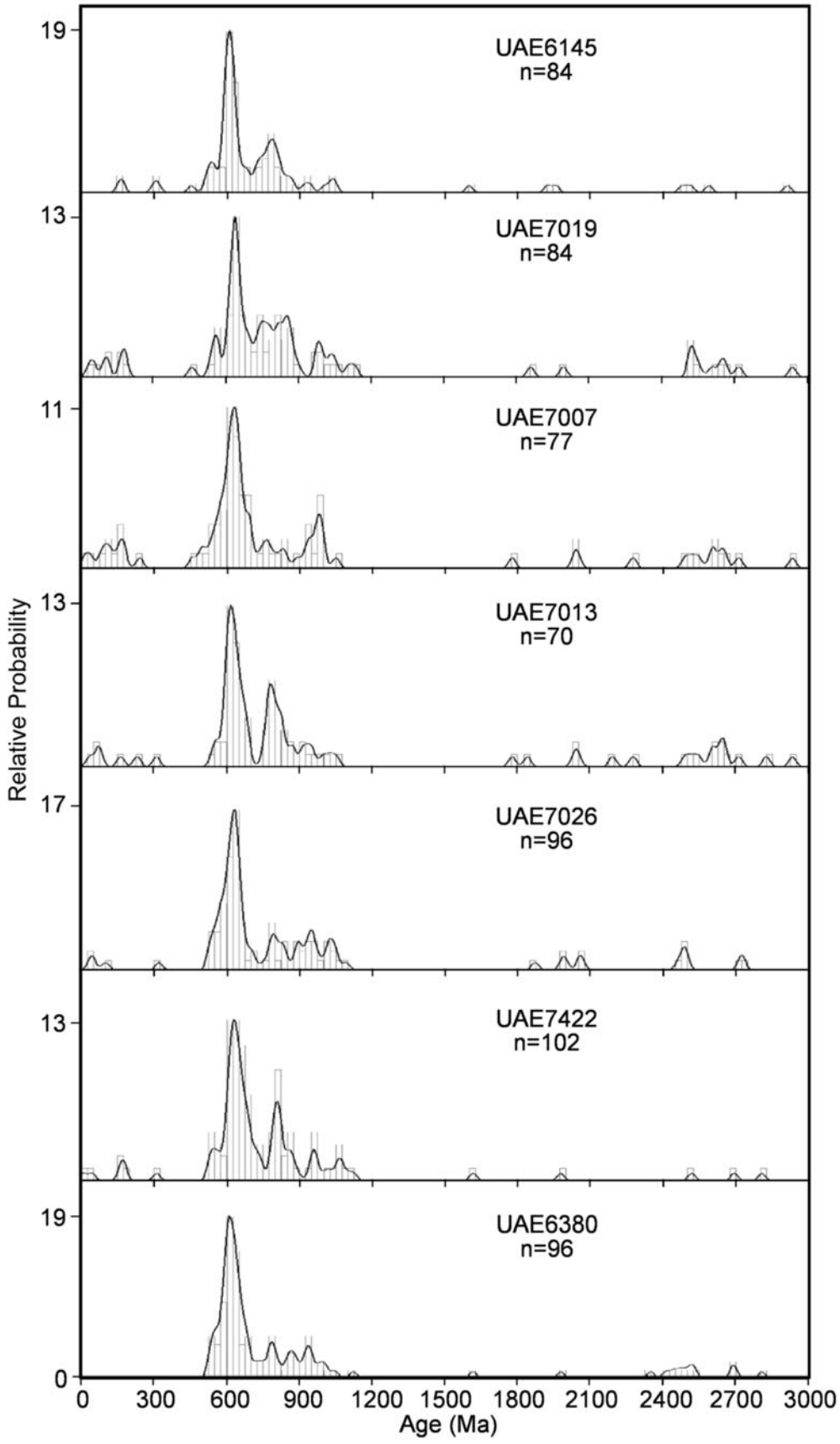

941

942 Fig. 10. Kernel Density Estimate and histograms for the detrital zircon U-Pb data; only data
943 within 10% discordance are shown.

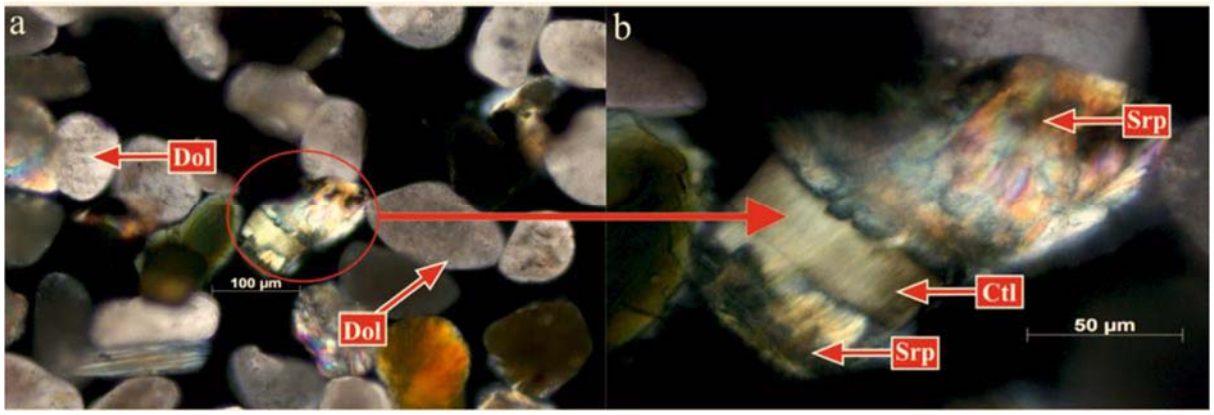

Fig. 11. Image of (**a**), detrital dolomite (Dol) and (**b**), detrital serpentine (Srp) with minor asbestiform [possibly chrysotile (Ctl)] vein.

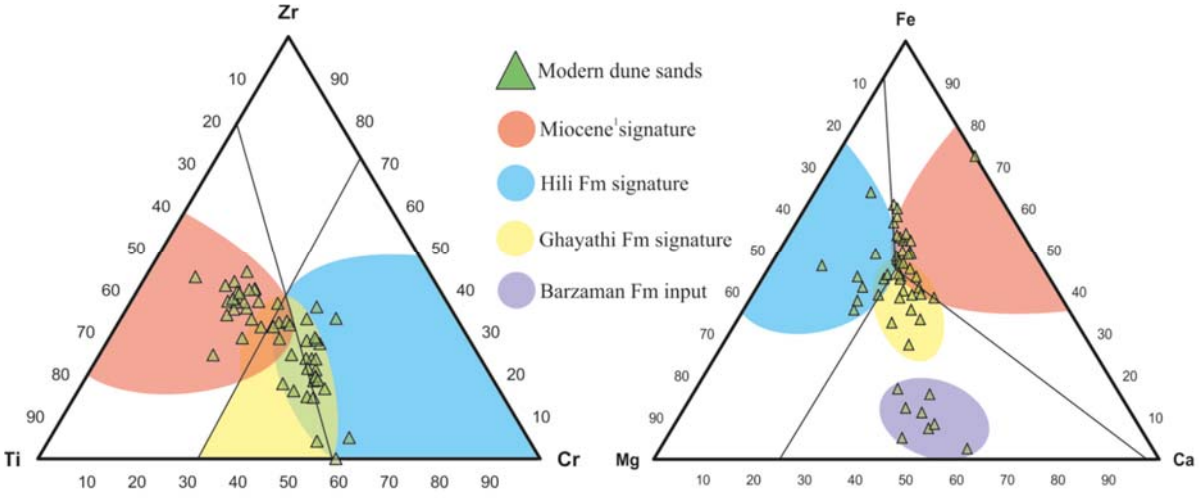

Fig. 12. Source plots for the modern dune sands based on (**a**) ultra-stable mineral geochemistry (USMG) and (**b**) less-stable mineral geochemistry (LSMG) data.

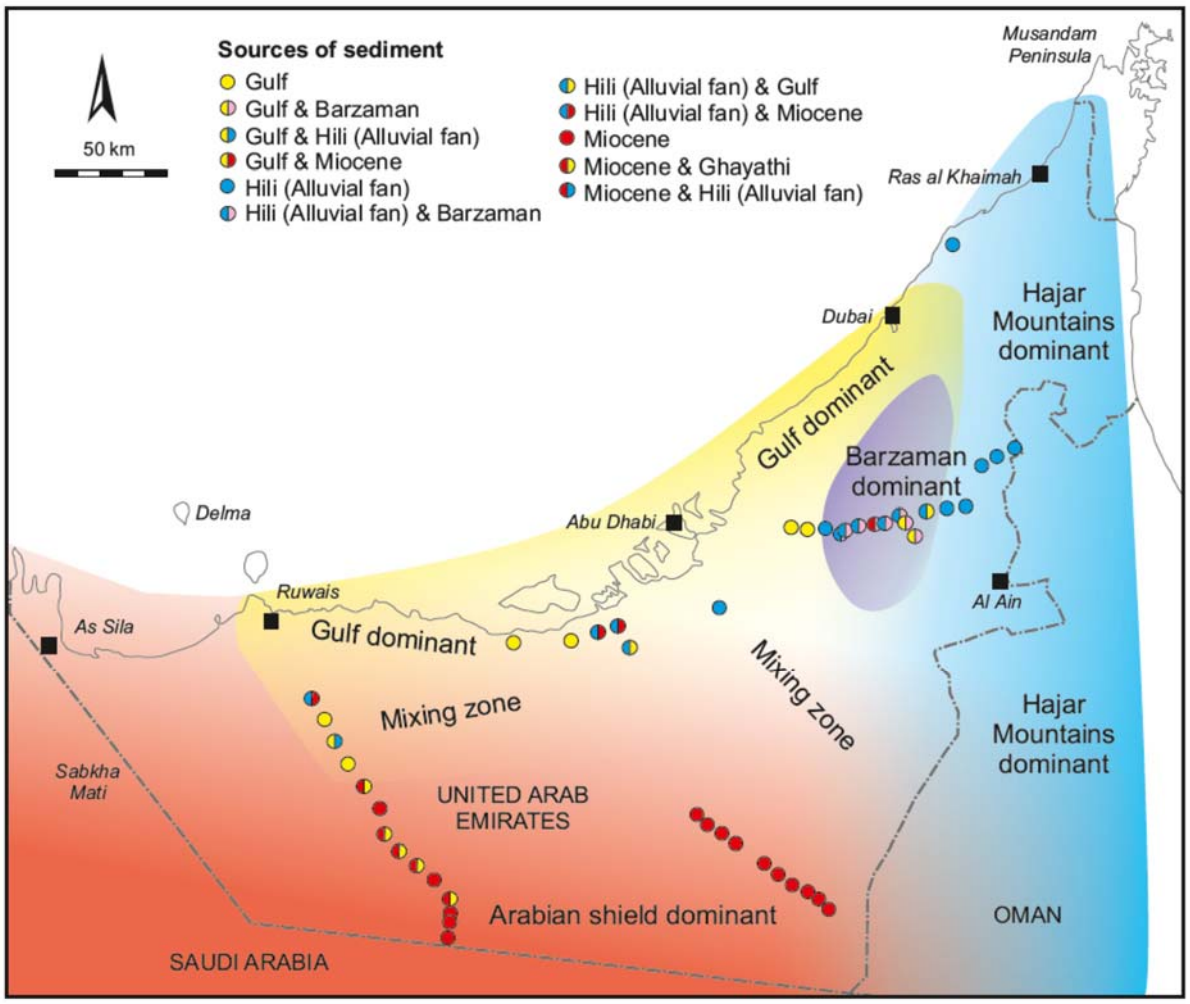

Fig. 13. Provenance of dune samples. Left hemisphere denotes the USMG component and right hemisphere the LSMG component. The colour shading denotes areas where particular dune sediment provenance signatures are dominant.

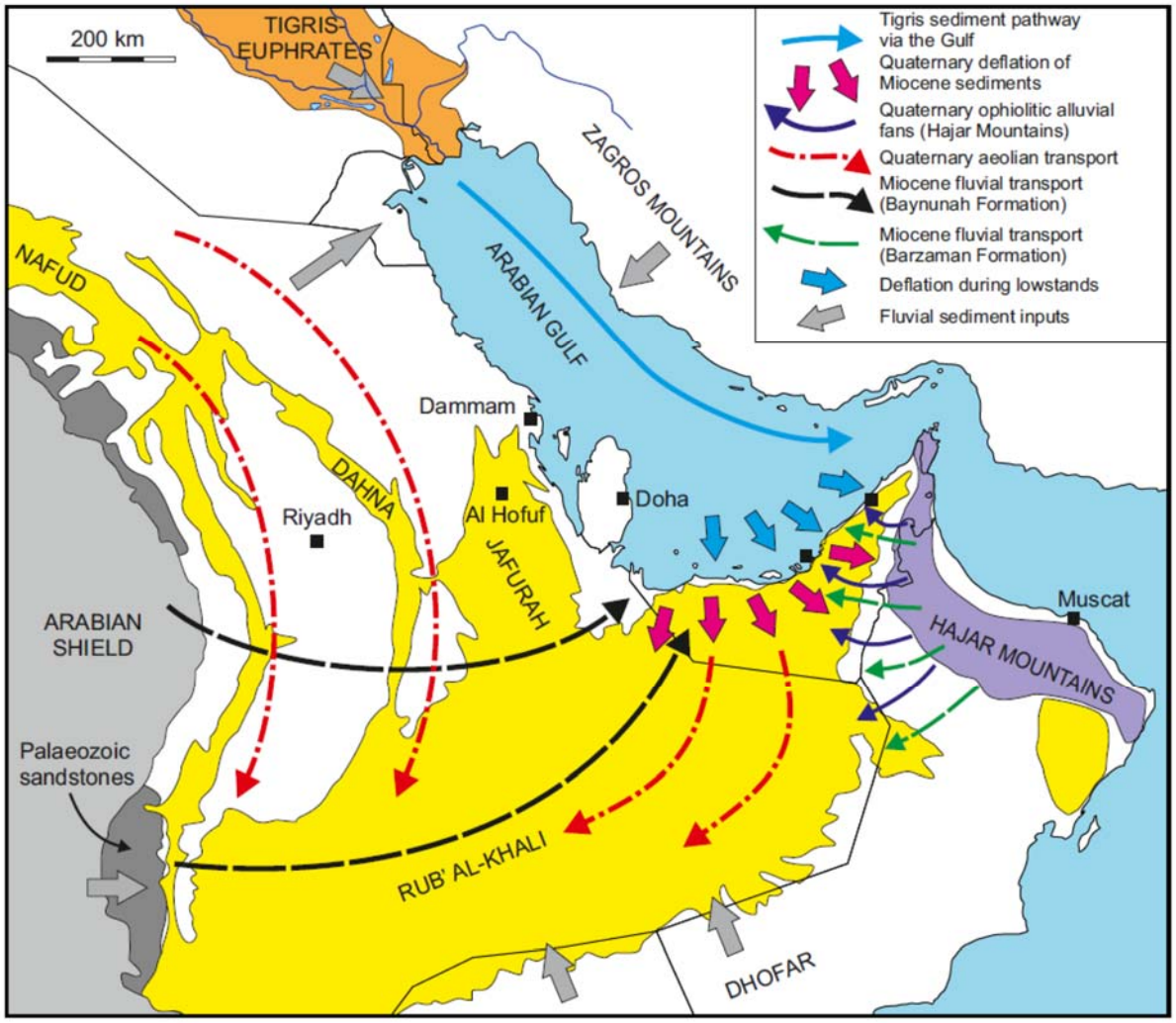

954

955 Fig. 14. Geological map of Arabia showing sediment routes transport routes during the
956 Miocene and the Quaternary.